# Synthesis, molecular modeling, and biological evaluation of novel RAD51 inhibitors

**ARTICLE** *in* EUROPEAN JOURNAL OF MEDICINAL CHEMISTRY · APRIL 2015

Impact Factor: 3.45 · DOI: 10.1016/j.ejmech.2015.04.021 · Source: PubMed



**7 AUTHORS**, INCLUDING:

Jiewen Zhu
University of California, Irvine
**8** PUBLICATIONS **110** CITATIONS
SEE PROFILE

A. Richard Chamberlin
University of California, Irvine
**141** PUBLICATIONS **5,395** CITATIONS
SEE PROFILE

European Journal of Medicinal Chemistry 96 (2015) 196–208

Contents lists available at ScienceDirect

European Journal of Medicinal Chemistry

journal homepage: http://www.elsevier.com/locate/ejmech

Original article

# Synthesis, molecular modeling, and biological evaluation of novel RAD51 inhibitors

Jiewen Zhu [a, 1], Hongyuan Chen [a, 1], Xuning Emily Guo [a, 1], Xiao-Long Qiu [a], Chun-Mei Hu [a, d], A. Richard Chamberlin [b], Wen-Hwa Lee [a, c, *]

[a] Department of Biological Chemistry, School of Medicine, USA
[b] Department of Pharmaceutical Sciences, University of California, Irvine, CA 92697, USA
[c] Graduate Institute of Clinical Medical Science, China Medical University, Taichung, Taiwan
[d] Taiwan Genomic Research Center, Academia Sinica, Taipei, Taiwan

ARTICLE INFO

*Article history:*
Received 11 February 2015
Received in revised form
6 April 2015
Accepted 8 April 2015
Available online 9 April 2015

*Keywords:*
RAD51 inhibitor
Indole alkaloid
Breast cancer
Triple-negative
QSAR
Synthesis

ABSTRACT

RAD51 recombinase plays a critical role for cancer cell proliferation and survival. Targeting RAD51 is therefore an attractive strategy for treating difficult-to-treat cancers, e.g. triple negative breast cancers which are often resistant to existing therapeutics. To this end, we have designed, synthesized and evaluated a panel of new RAD51 inhibitors, denoted IBR compounds. Among these compounds, we have identified a novel small molecule RAD51 inhibitor, **IBR120**, which exhibited a 4.8-fold improved growth inhibition activity in triple negative human breast cancer cell line MBA-MD-468. **IBR120** also inhibited the proliferation of a broad spectrum of other cancer cell types. Approximately 10-fold difference between the $IC_{50}$ values in normal and cancer cells were observed. Moreover, **IBR120** was capable of disrupting RAD51 multimerization, impairing homologous recombination repair, and inducing apoptotic cell death. Therefore, these novel RAD51 inhibitors may serve as potential candidates for the development of pharmaceutical strategies against difficult-to-treat cancers.



## 1. Introduction

Targeting DNA damage repair pathway as a novel means of treating cancer, especially difficult-to-treat cancers, has attracted much attention in the past a few years. Homologous recombination (HR) is one of the most prominent repair pathways and is required for cancer cells to undergo continuous proliferation under stress. Therefore, various efforts have been taken to inhibit or modulate this pathway, in the hope of rendering cancer cells vulnerable [1–4]. As one of the key players in HR, RAD51 is essential for DNA repair, proliferation and survival. RAD51 protein level is elevated in many cancer cells, contributing to their resistance to chemotherapy and the continuous cell proliferation [5–14]. Therefore, RAD51 inhibition has been pursued by several groups in search of a novel potential treatment for difficult-to-treat-cancers [2,3,15].

Recently, our group identified and validated a small molecule synthetic alkaloid, named **IBR2** (Fig. 1), which showed interesting RAD51 inhibition activities both *in vitro* and *in vivo* [15]. RAD51 was rapidly degraded in **IBR2**-treated cancer cells, and the homologous recombination repair was impaired, subsequently leading to cell death. Therefore, **IBR2** represents a novel class of direct and specific RAD51 inhibitors [1–3,15]. The $IC_{50}$ values of the original **IBR2** were in the range of 12–20 μM for most tested cancer cell lines. Its molecular scaffold contains a chiral center and the structure-activity relationship of this chirality has not been explored in our previous studies. It is well accepted that the interaction between chiral molecules and biological systems can provide more

*Abbreviations:* DMAP, 4,4-dimethylaminopyridine; XTT, sodium 3′-[1-(phenylaminocarbonyl)-3,4-tetrazolium]-bis(4-methoxy-6-nitro-) benzene sulfonate; IBR, RAD51 inhibitor.

* Corresponding author. Department of Biological Chemistry, School of Medicine, University of California, Irvine, 240 Med Sci D, Irvine, CA 92697, USA.
*E-mail address:* whlee@uci.edu (W.-H. Lee).

[1] These authors contributed equally to this work. HC, XLQ, and JZ designed, synthesized, and characterized all compounds under the guidance of ARC; XEG and CMH performed XTT assay and HR assay; JZ performed the gel filtration assay, QSAR analysis, and molecular modeling. JZ and WHL wrote the paper with inputs from all authors.

http://dx.doi.org/10.1016/j.ejmech.2015.04.021
0223-5234/

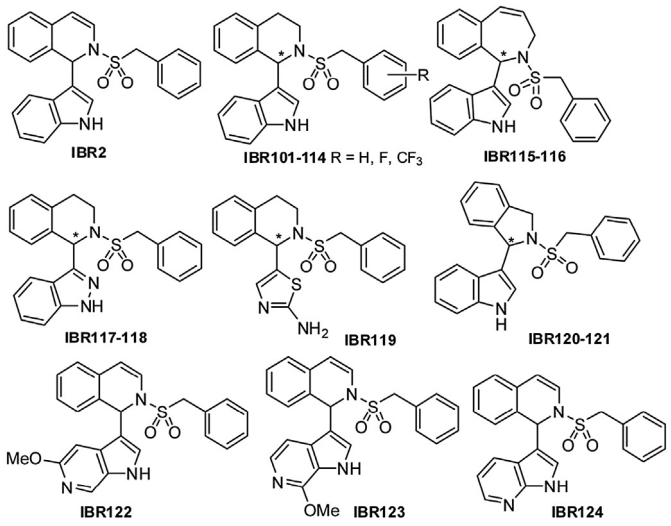


**Fig. 1.** Structures of **IBR2** and its analogues **IBR101–124**.

mechanistic insight and important clues for drug discovery and development [16]. Therefore, we sought to develop efficient and stereo-selective synthetic routes such that more potent analogues can be identified [17]. In this report, several types of **IBR2** analogues **IBR101–124** were designed, synthesized, modeled, and biologically evaluated. These new compounds constitute a focused compound library representing a diversity of modified scaffold or substituents (Fig. 1). As a result, a 4.8-fold improved RAD51 inhibitor was identified, which was able to inhibit the growth of triple-negative breast cancer cells and a panel of other malignancies. This finding may provide support for innovative methods and developments in cancer treatment.

## 2. Results and discussion

### 2.1. Synthesis of *IBR2* analogues

1,2,3,4-tetrahydroisoquinoline indole alkaloids **IBR101–114** were stereoselectively synthesized by the addition of *N*-Boc-3-bromo-indole **1** to the chiral benzylidene sulfinamide **2** as key steps [17]. 2,3-dihydro-1*H*-benzo[*c*]azepine analogues **IBR115–116** were stereoselectively synthesized using the bifunctional cinchona alkaloid-thiourea catalyzed addition of unprotected indole **3** to the sulfonyl amide **4** (Scheme 1) [17,18].

Synthesis of optically pure indazole derivative **IBR117** embarked on the reaction of the chiral benzylidene sulfinamide **2** [17] and 3-Bromoindazole **5**. The desired indazolylated adduct **6** was obtained in medium yield (43%) and diastereoselectivity (65% *dr*) (Scheme 2) [19]. Protection of **6** with $Boc_2O$ gave compounds **7** and **8** in 66% and 14% yields, respectively. To our delight, the diastereoisomers **7** and **8** could be readily separated by silica gel column chromatography. Then, starting with chiral sulfinamide **8**, HCl-mediated removal of the *tert*-butanesulfinyl group provided the amine product **9** in 90% yield. Subjecting the amine **9** to Pd/C-catalyzed hydrogenation followed by exposure of the resultant alcohol to CbzCl/DIPEA gave the compound **10** in 61% yield over 2 steps. Alcohol **10** was further mesylated to give compound **11** in 91% yield. Once hydrogenation of the mesylate **11** was carried out with Pd/C as catalyst in MeOH, the desired cyclic amine **12** was isolated in 94% yield, which led directly to **IBR117** in 61% yield via deprotection with NaOMe/MeOH and subsequent benzylsulfonylation. Utilizing similar reaction procedures, the *S* configuration indazole derivative **IBR118** was also prepared starting from chiral sulfinamide **7** in 37% yield over 5 steps (Scheme 3).

Chiral thiazolylamine derivative **IBR119** was synthesized starting from *N*-Boc-2-amino-5-bromothiazole **17** and chiral benzylidene sulfinamide **2** (Scheme 4). Addition proceeded well by treatment of compound **2** with *N*-Boc-2-amino-5-lithiothiazole (prepared *in situ* via reaction of 17 with *n*-BuLi) at −78 °C, and the desired sulfinamides **18** and **19** were provided in 39% yield with medium diastereoselectivity (59% *dr*). Diastereoisomers **18** and **19** (1:4 isolated molar ratio) were then successfully separated through silica gel chromatography (isolated yield: 8% and 31%, respectively). The major diastereomer compound **19** was chosen for further modification. *tert*-Butanesulfinyl group of **19** was removed by treatment with 4 M HCl in dioxane and the amine **20** was obtained in almost quantitative yield. Benzylsulfonylation of **20** gave compound **21** in 97% yield, which was subjected to Pd/C-catalyzed hydrogenation to afford the alcohol **22** in 80% yield. Mesylation of **22** by treatment with MsCl/DMAP/DIPEA followed by exposure of resultant mesylate to KHDMS in THF furnished the desired cyclic compound **23**. Synthesis of **IBR119** was finally accomplished via TFA-mediated removal of Boc protecting group in **23**.

Synthesis of isoindolinyl derivative **IBR120** started from the indole-derivated compound **24**, which was prepared according to our previous report [17,18]. A direct $OsO_4$–$NaIO_4$ mediated oxidative cleavage reaction on unprotected compound **24** in the presence of 2, 6-lutidine [20] was carried out, followed by reduction with $NaBH_4$ and resulted in alcohol **25** (82%). Alcohol **25** was then treated with mesyl chloride and an appropriate base in DCM to give the corresponding mesylate, which was used as an intermediate for the following cyclisation reaction to form **IBR120**. Our first attempt on cyclization of alcohol **25** using KHMDS as a base in THF gave a racemic product. Reaction conditions with milder bases were then investigated (Table S1 in Supporting information). Reactions with $Et_3N$ in DCM at r.t. or in dioxane under reflux did not facilitate the conversion. The use of $K_2CO_3$ in MeOH gave racemic cyclization product in 42% yield. Finally, with Hünig's base in acetonitrile, the desired product **IBR120** was obtained in 53% yield with >95% ee (Scheme 5). Utilizing the similar reaction procedures, the *S* configuration isomer **IBR121** was also prepared starting from the indole-derivated compound **26** (Scheme 6). Chiral HPLC analysis confirmed high enantiomeric purities of **IBR120** and **IBR121** (See Figs. S1–S3 in Supporting Information for representative HPLC profiles).

To explore possible effects of other indole bioisosteres on the bioactivity, racemic azaindole derivatives **IBR122–124** were synthesized using a facile one-pot synthetic method as described in our previous report [15], starting from azaindoles **27**, **28**, and **29**, respectively (Scheme 7).

### 2.2. *IBR2* analogues inhibit growth of triple-negative human breast cancer

Triple-negative breast cancer is often easy to metastasize and difficult to treat using existing therapeutics [21,22]. As a broad spectrum anti-cancer agent, **IBR2** was able to inhibit a number of difficult-to-treat cancers [15]. To test the possibility of inhibiting triple-negative breast cancer, we screened the newly synthesized **IBR2** analogues **IBR101–124** of their growth inhibition abilities using an XTT assay. As shown in Table 1, most of these synthetic **IBR2** analogues can inhibit the growth of triple-negative human breast cancer cell line MBA-MD-468.

We found that the half inhibitory concentrations ($IC_{50}$) of 1,2,3,4-tetrahydroisoquinoline analogues **IBR101, 102, 103, 105,**

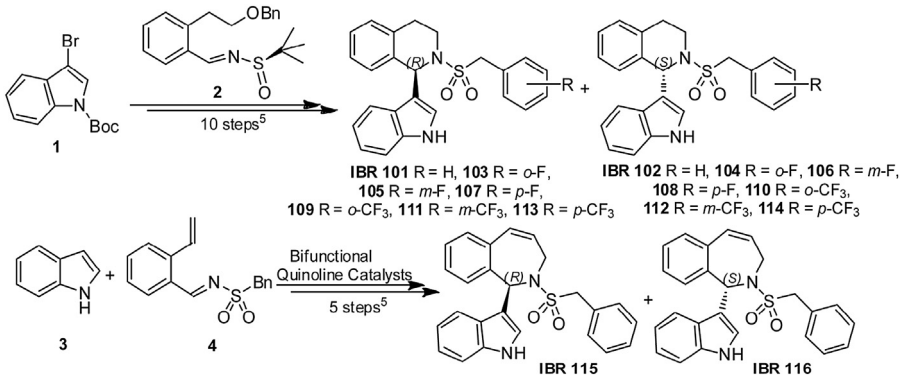


**Scheme 1.** Synthesis of **IBR101–116** [17].

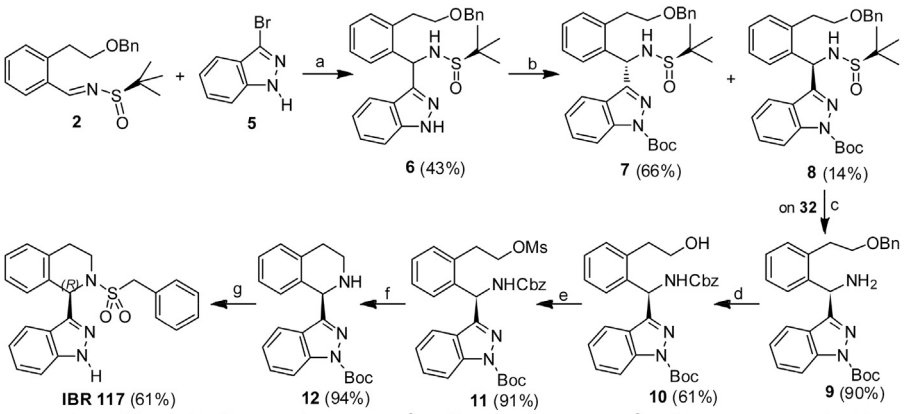


[a] Reagent and conditions: (a) (i) *n*-BuLi, THF, -78 °C; (ii) *t*-BuLi, THF, -78 °C; (b) $Boc_2O$, $CH_2Cl_2$; (c) 4M HCl in dioxane, MeOH, rt.; (d) (i) Pd / C, $H_2$ (1 atm), 4M HCl in dioxane, MeOH, rt.; (ii) CbzCl, DIPEA, $CH_2Cl_2$, 0 °C; (e) MsCl, DIPEA,$CH_2Cl_2$, rt; (f) Pd / C, MeOH, $H_2$ (1 atm), rt; (g) (i) NaOMe, MeOH, rt.; (ii) $BnSO_2Cl$, $CH_2Cl_2$, DIPEA, 0°C.

**Scheme 2.** Synthesis of **IBR117**. Reagent and conditions: (a) (i) *n*-BuLi, THF, −78 °C; (ii) *t*-BuLi, THF, −78 °C; (b) $Boc_2O$, $CH_2Cl_2$; (c) 4 M HCl in dioxane, MeOH, rt.; (d) (i) Pd/C, $H_2$ (1 atm), 4 M HCl in dioxane, MeOH, rt.; (ii) CbzCl, DIPEA, $CH_2Cl_2$, 0 °C; (e) MsCl, DIPEA,$CH_2Cl_2$, rt; (f) Pd/C, MeOH, $H_2$ (1 atm), rt; (g) (i) NaOMe, MeOH, rt.; (ii) $BnSO_2Cl$, $CH_2Cl_2$, DIPEA, 0 °C.

**107, 109, 111, 113, 118**, 2,3-dihydro-1*H*-benzo[*c*]azepine analogue **IBR115**, and 1,2-dihydroisoquinoline analogue **IBR122** were slightly lower than that of the parental compound **IBR2**; while 1,2,3,4-tetrahydroisoquinoline analogue **IBR117**, isoindoline analogue **IBR120**, and 1,2-dihydroisoquinoline analogues **IBR123, 124** were significantly lower than that of **IBR2**. In all the successfully synthesized enantiomers, the *R* configuration consistently exhibited better bioactivity than the *S* configuration. Among all these analogues, **IBR120** exhibited a 4.8-fold increase in activity ($IC_{50}$ = 3.1 μM), followed by **IBR124, 123** and **117**, with 1.6–2.4-fold increase in activities ($IC_{50}$ = 6.2, 6.3, 9.5 μM, respectively), compared to the parental compound **IBR2** ($IC_{50}$ = 14.8 μM).

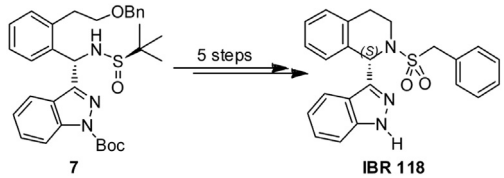


**Scheme 3.** Synthesis of **IBR118**.

### 2.3. *IBR120* inhibits a panel of cancer cell lines growth

We then tested the best analogue **IBR120** on the growth inhibition of a panel of cancer cell lines using XTT assay. These cell lines included human Chronic Myelogenous Leukemia cell line K562, human breast cancer cell lines MCF7, MDA-MB-231, MDA-MB-361, MDA-MB-435, MDA-MB-468, Hs578-T, and T47D, human Osteosarcoma cell line U2OS, human Glioblastoma cell line T98G, human Cervical Cancer cell line HeLa, as well as human mammary gland normal epithelial cell line MCF10A (normal control). As shown in Table 2, while essentially nontoxic to the normal cell line MCF10A ($IC_{50}$ > 30 μM), **IBR120** exhibited killing effect in most tested cancer cell lines with $IC_{50}$ values in low micromolar range (3–5 μM). This approximately 10-fold difference between the $IC_{50}$ values in normal and cancer cells demonstrates a potential therapeutic window for future drug development.

### 2.4. Molecular docking model

We have previously shown that the phenylalanine binding site on the RAD51 core domain was responsible for **IBR2** binding [15]. Blocking of this site inhibits RAD51 multimerization and leads to deficiencies in DNA repair; while mutation in the center of this site abolishes the binding [15]. ICM software was employed to prepare

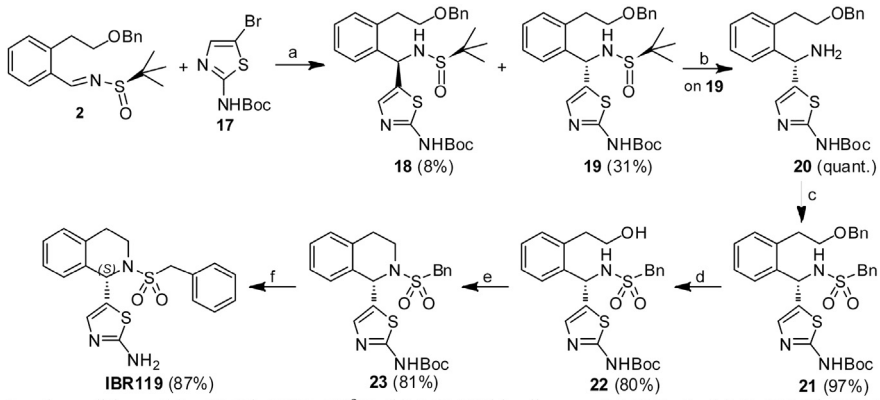


[a] Reagent and conditions: (a) n-BuLi, THF, -78°C; (b) 4 M HCl in dioxane, MeOH, rt.; (c) $BnSO_2Cl$, $CH_2Cl_2$, DMAP, DIPEA; (d) Pd / C, $H_2$ (1 atm), 4 M HCl in dioxane, MeOH; (e) (i) MsCl, DMAP, DIPEA, $CH_2Cl_2$, 0 °C to rt.; (ii) KHMDS, THF, 0 °C; (f) TFA, $CH_2Cl_2$, rt.

**Scheme 4.** Synthesis of **IBR119**. Reagent and conditions: (a) n-BuLi, THF, −78 °C; (b) 4 M HCl in dioxane, MeOH, rt.; (c) $BnSO_2Cl$, $CH_2Cl_2$, DMAP, DIPEA; (d) Pd/C, $H_2$ (1 atm), 4 M HCl in dioxane, MeOH; (e) (i) MsCl, DMAP, DIPEA, $CH_2Cl_2$, 0 °C to rt.; (ii) KHMDS, THF, 0 °C; (f) TFA, $CH_2Cl_2$, rt.

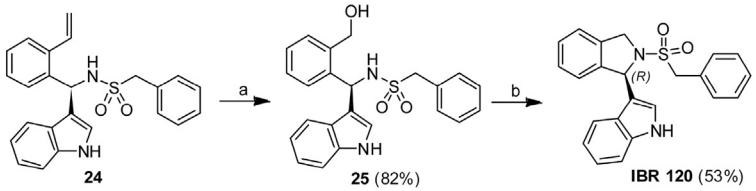


[a] Reagent and conditions: (a) (i) 2,6-lutidine, $OsO_4$, $NaIO_4$, Dioxane, $H_2O$, rt.; (ii) $NaBH_4$, THF, MeOH, 0°C to rt.; (b) (i) MsCl, $CH_2Cl_2$, $Et_3N$; (ii) DIPEA, MeCN.

**Scheme 5.** Synthesis of **IBR120** Reagent and conditions. (a) (i) 2,6-lutidine, $OsO_4$, $NaIO_4$, Dioxane, $H_2O$, rt.; (ii) $NaBH_4$, THF, MeOH, 0 °C to rt.; (b) (i) MsCl, $CH_2Cl_2$, $Et_3N$; (ii) DIPEA, MeCN.

the structures of RAD51 core domain, and to perform the molecular docking studies with IBR2 analogues. The crystal structure of human RAD51 in complex with BRC4 peptide (PDB No. 1N0W) [24] was chosen for molecular docking studies. Initially a docking box containing all the atoms of RAD51 residues within 5 Å distance from the BRC4 peptide in 1N0W was used; and a "blind docking" procedure was performed using **IBR2** as probe. Then the docking box was fixed and used for all docking studies with **IBR2** analogues; the amino acid residues within the box contain RAD51 residues M158, Y159, I160, F167, P168, L171, S183, V185, L186, D187, N188, V189, A190, Y191, A192, R193, A194, F195, H199, Q202, L203, L204, Y205, Q206, A207, S208, A209, M210, V212, E213, Y216, L219, R247, R250, M251, L252, R254, L255, E258, F259. Molecular docking was then performed following rigid docking protocols; docking scores were collected and conformational analysis was performed based on the results.

Many of the residues in the binding site are hydrophobic and therefore provides hydrophobic surface for interacting with the aromatic ring systems of the IBR compounds. Three potential hydrogen bonding sites were identified between **IBR120** and RAD51 residues V189, Y191, and Q206. The distance between the indole nitrogen atom and the backbone carbonyl oxygen of V189 was 3.3 Å, suggesting a hydrogen bond of moderate strength may be involved in the binding. This notion is partly consistent with our previous finding that methylation of the indolyl nitrogen resulted in loss of activity [15]. An alternative explanation for the loss of activity in the N-methylated analogue could be that the methyl group might introduce unfavorable steric interaction with the corresponding amino acid residues on RAD51. Moreover, both of the sulfonyl oxygen atoms seem to be involved in weak hydrogen bonding, which could explain the observed loss of function when changing the sulphonyl into carbonyl group as our previous results showed [15] (Fig. 2).

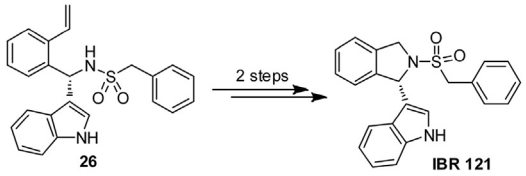


**Scheme 6.** Synthesis of **IBR121**.

### 2.5. Quantitative structure activity relationship (QSAR) analysis

The phenyl moiety of **IBR2** is situated in a spatially confined environment on RAD51 protein [15]. In this work, we have modified the indolyl and isoquinoline moieties of **IBR2** to further explore the structure-activity relationship. Our new IBR compounds described in this work covered the following structural diversity of interest: (1) different bioisosteres for replacing the indolyl ring, (2) chiral center of **IBR2** analogues, and (3) variable sizes of the central ring.

By modifying indole moiety to various bioisosteres, a potentially favorable modification site was identified. We found that compared with **IBR2**, **IBR123** and **124** showed more than 2-fold increase of activity; and both **IBR123** and **124** have included a potential

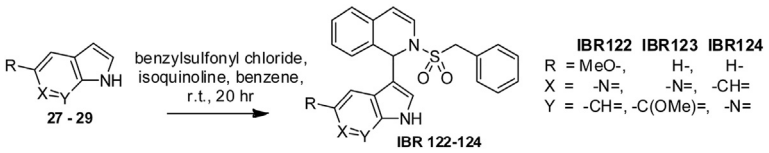


**Scheme 7.** Synthesis of **IBR122–124** [15].

hydrogen bond acceptor at the 7-position of the indolyl ring, suggesting further improvement could be made by utilizing this feature. Second, the growth inhibition assay results indicated that, compared with *S* isomers (average $pIC_{50} = 4.70$), the *R* isomers (average $pIC_{50} = 4.96$) are generally more active (Student's *t*-test, $p = 0.0047$) as summarized in Fig. 3A. Moreover, increasing the central ring size from six to seven resulted in minimal change of activity of the *R* isomer (**IBR115**), but almost complete loss of function in the *S* isomer (**IBR116**). Interestingly, decreasing the central ring size from six to five resulted in more than 4-fold increase of activity (**IBR120**). If we assume that other confounding factors, such as assay variability, solubility differences, or variations in protein binding, remain similar among all the compound structures, these observed effects on activity could be viewed as results of certain molecular recognition driven events. As we have discussed in previous sections, the docked conformation of **IBR120** indeed showed several favorable features of binding.

To better understand how these structural factors might have invoked such changes in activity, we decided to further look into the optimal docked conformations of all compounds. We hypothesized that the various sizes of the ring and substituent could result in differences in the optimal orientations of the indolyl, phenyl, and sulphonyl groups. This orientation can be readily quantified with a dihedral angle in the docking model (C–C–N–S, as shown in Fig. 3B, inset). A cluster analysis (k-means, $k = 2$) of this dihedral angle with regard to the $IC_{50}$'s indicated that the dihedral angles clustered around 75–100° usually correlated with better activity; while the dihedral angles of −60~-110° correlated with poorer activity (Fig. 3B). Therefore the combined conformational effect elicited by the ring size and substituents determines the activity of a certain compound, at least in part.

We then attempted to build a predicative multivariate linear regression model based on the above observations obtained from all the synthesized chiral and racemic compounds. First, the molecules were divided into a test set (9 compounds) and a training set (16 compounds) using a random number generator to minimize potential bias. We then chose a handful of molecular descriptors (Molecular Weight, LogP, LogS, Polar Surface Area, Molecular Volume, Heat of Formation) to account for the difference in the physicochemical properties of the small molecules, and docking scores as indicators of overall binding capacity with RAD51. And we generated a first predicative model (Multiple R-squared: 0.77, Adjusted R-squared: 0.57, p-value: 0.039, see Fig. S4 in Supporting Information). Next, based on the above exploratory analysis, we then included two extra parameters (dihedral angle and chirality) to account for the important conformational preference as we discussed above; and a much improved predicative model was obtained (Multiple R-squared: 0.98, Adjusted R-squared: 0.96, p-value: 0.0001, Fig. 3C, Training Set). Using this model, we were able to predict the growth inhibition activity of most compounds in the test tests within 95% confidence interval (Fig. 3D, Testing Set).

### 2.6. *IBR120* inhibits RAD51 multimerization

On the RAD51 core domain, a hydrophobic pocket formed between β-strand B3 and α-helix A4 of RAD51 [24] is critical for RAD51 multimerization, which is also responsible for **IBR2** competitive binding [15]. Therefore, analogous IBR compounds were expected to inhibit RAD51 multimerization. To demonstrate that **IBR120** can indeed do this, we compared the gel filtration profile of RAD51 multimerization in the presence of **IBR120** or vehicle (DMSO) alone. In the presence of **IBR120**, the RAD51 elution profile exhibited a major peak consistent with the molecular weight of a monomer, while in the absence of **IBR120**, the majority of RAD51 formed multimers (Fig. 4), indicating that **IBR120**, similar to **IBR2**, can inhibit RAD51 multimerization.

### 2.7. *IBR120* inhibits homologous recombination (HR) repair

Inhibition of RAD51 function will lead to failure in HR repair. To test this possibility, we used an I-SceI inducible gene conversion assay that measures the DNA double strand break repair frequency by detecting successful restoration of a fluorescent GFP from the repair substrate DR-GFP [15,25]. DR-GFP, consisting of two nonfluorescent GFP derivatives, SceGFP and iGFP, was first stably integrated into HeLa cells. Upon I-SceI expression by transient transfection for 24 h to induce DSBs, cells were treated with DMSO, 10 or 20 μM of **IBR120** or **IBR2** for another 24 h and the GFP positive population resulting from successful recombination was measured by flow cytometry. As shown in Fig. 5, the HR frequency was significantly reduced after **IBR120** treatment in a dose dependent

**Table 1**
**IBR2** analogues inhibit the growth of the triple-negative human breast cancer cell line MDA-MB-468.

| Compound | $IC_{50}$ (μM) | Compound | $IC_{50}$ (μM) | Compound | $IC_{50}$ (μM) |
|---|---|---|---|---|---|
| IBR2 (*rac*) | *14.8* | | | | |
| IBR101 (*R*) | 11.7 | IBR109 (*R*) | 14.8 | IBR117 (*R*) | 9.5 |
| IBR102 (*S*) | 13.2 | IBR110 (*S*) | 16.7 | IBR118 (*S*) | 14.3 |
| IBR103 (*R*) | 12.7 | IBR111 (*R*) | 11.1 | IBR119 (*S*) | >25 |
| IBR104 (*S*) | 19.2 | IBR112 (*S*) | 22.2 | IBR120 (*R*) | **3.1** |
| IBR105 (*R*) | 14.2 | IBR113 (*R*) | 13.6 | IBR121 (*S*) | >12 |
| IBR106 (*S*) | 17.2 | IBR114 (*S*) | 20.7 | IBR122 (*rac*) | 12.7 |
| IBR107 (*R*) | 11.2 | IBR115 (*R*) | 14.7 | IBR123 (*rac*) | 6.3 |
| IBR108 (*S*) | 25.7 | IBR116 (*S*) | >50 | IBR124 (*rac*) | 6.2 |

To highlight the improvement of activity, the $IC_{50}$ value of the parent compound **IBR2** is shown in italic, and the $IC_{50}$ value of **IBR120** is shown in bold.

**Table 2**
Inhibition activity of **IBR120** on a panel of cancer cell lines.

| Cell line | Cell type [23] | $IC_{50}$ (μM) | |
|---|---|---|---|
| K562 | Chronic myelogenous leukemia | 3.6 | ±0.7 |
| MCF7 | Mammary gland adenocarcinoma | 3.1 | ±0.2 |
| MDA-MB-231 | Mammary gland adenocarcinoma | 3.5 | ±0.4 |
| MDA-MB-361 | Mammary gland adenocarcinoma | 4.5 | ±0.7 |
| MDA-MB-468 | Mammary gland adenocarcinoma | 3.1 | ±0.4 |
| MDA-MB-435 | Melanoma/mammary gland ductal carcinoma | 4.0 | ±0.7 |
| Hs578-T | Mammary gland carcinoma | 4.9 | ±1.0 |
| T47D | Mammary gland ductal carcinoma | 6.3 | ±1.5 |
| U2OS | Osteosarcoma | 4.7 | ±0.5 |
| T98G | Glioblastoma multiforme | 9.5 | ±0.9 |
| HeLa | Cervix adenocarcinoma | 3.6 | ±0.6 |
| MCF10A | Mammary gland, normal epithelial cell line | >30 | |

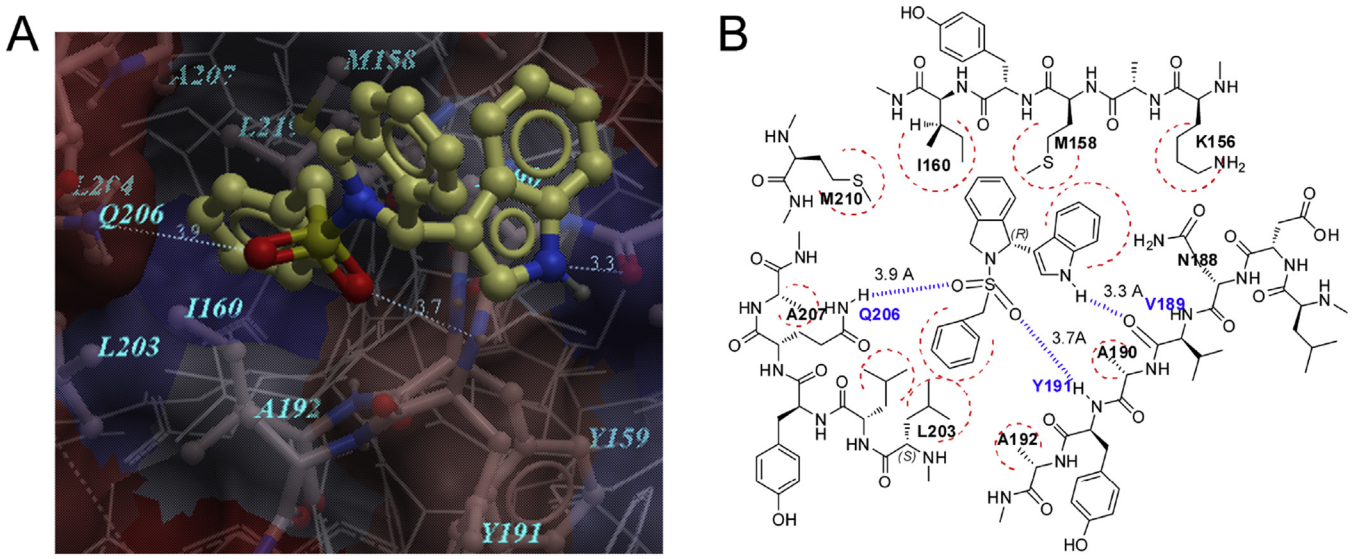


**Fig. 2.** RAD51-**IBR120** Docking Model. (A) Binding conformation with lowest energy. RAD51 residues within 5 Å of docked **IBR120** are labeled in cyan. Potential hydrogen bonds are labeled in dashed lines. RAD51 protein is shown as transparent surface according to hydrophobicity, with ball-and-stick model indicating docking site. (B) Schematic of contributing intermolecular interactions between RAD51 and **IBR120**. Potential hydrogen bonds are shown in blue. N–H–O distances (Å) are indicated. Hydrophobic surfaces are marked with red dashed curves. (For interpretation of the references to colour in this figure legend, the reader is referred to the web version of this article.)

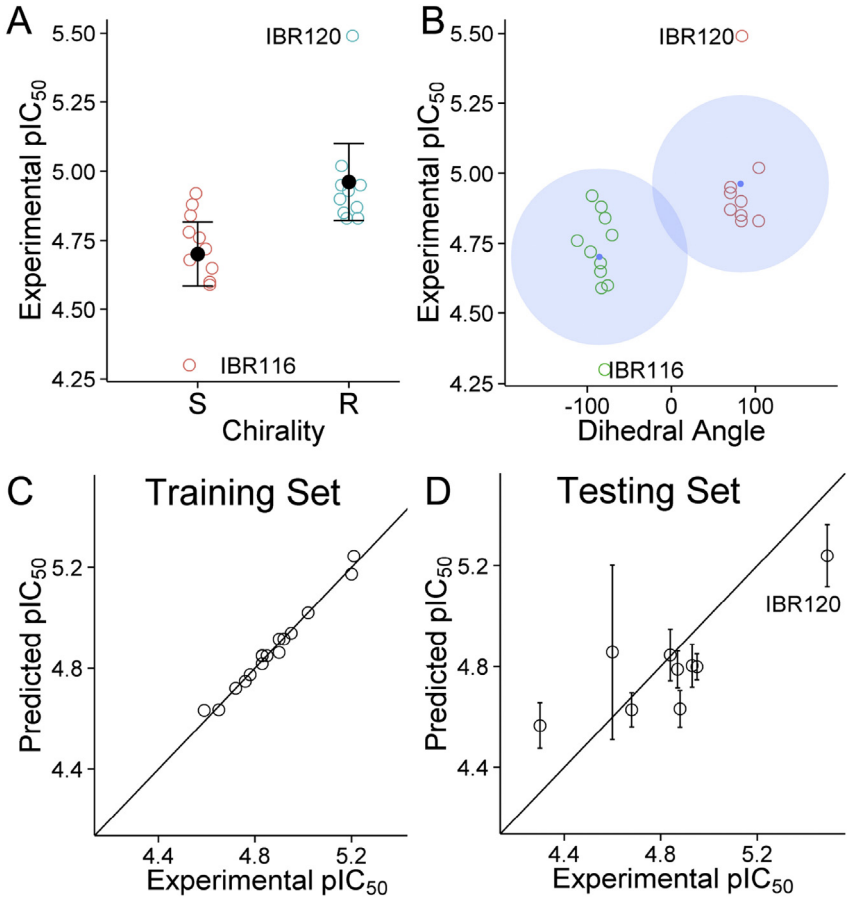


**Fig. 3.** Structural Activity Relationship. (A) *R*-configuration has better activity than *S*-configuration (two-tailed *t*-test, $p < 0.01$). Inset: star (*) shows the chiral center in **IBR120**. (B) Correlation between activity and dihedral angle in all 25 compounds. Cluster centers were obtained using K-means clustering algorithm (k = 2). Inset showing the dihedral angle formed by C–C–N–S in IBR120 (shown as bold bonds). (C) Predictive Multivariate linear model derived from the training set (pIC50 ~ (6.15 ± 1.73) - (0.02 ± 0.01) * MolWeight − (0.45 ± 0.12) * MolLogP − (0.20 ± 0.05) * MolLogS + (0.01 ± 0.01) * MolPSA + (0.018 ± 0.005) * MolVol − (0.006 ± 0.003) * MoldHf − (0.025 ± 0.005) * Score + (0.0021 ± 0.0007) * DihedralAngle − (0.08 ± 0.06) * Chirality), Residual standard error: 0.034 on 6 degrees of freedom, Multiple R-squared: 0.98, Adjusted R-squared: 0.96, p-value: 0.0001. (D) Prediction result on the test sets in comparison with experimental data (see Table S2 in Supporting information for full data set).

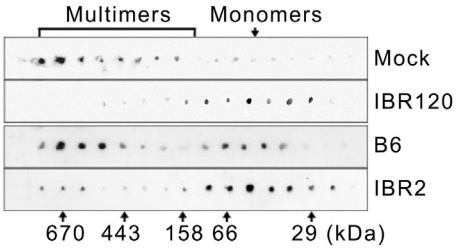


**Fig. 4. IBR120** inhibits RAD51 multimerization. Lanes **B6** and **IBR2** were adapted from our previous work [15]. The multimers and monomers were separated on a 2.4 ml Superdex 200 PC 3.2/30 size exclusion column and detected using monoclonal anti-RAD51 antibody, as described in method.

manner. Compared with **IBR2** treatment, **IBR120** treatment consistently led to greater depression of HR repair activity.

## 3. Conclusion

In summary, we have developed several stereoselective synthetic routes to synthesize chiral IBR2 analogues. One route featured the addition of N-Boc-3-bromo-indole **1**, 3-bromoindazole **5** and N-Boc-2-amino-5-bromothiazole **17** to the benzylidene sulfinamide **2** provided the separable diastereoisomers in medium to good yields. The biological assays and QSAR studies clearly demonstrated that *R* configuration exhibited improved bioactivity than *S* configuration, and the 5-membered central ring system proves to be the most active; these effects can be structurally correlated to the fine-tuning of the orientation of the two aromatic groups. As a result, these modifications led to more than 4-fold increase of growth inhibition activity in a panel of cancer cells, providing a significant milestone towards better RAD51 inhibitors.

Our synthetic scheme for most of the described IBR compounds relies on the stereoselective arylation of chiral benzylidene sulfinamide **2**, using *in situ* generated lithium reagent, followed by separation of diastereomers, removal of chiral auxiliary group, and further modifications thereafter. This route calls for a total of 6–10 steps of conversions to obtain the target molecules, in which a chromatographic separation of diastereomers is indispensable. These undesirable hurdles can be overcome in further optimization of the synthetic route. Indeed, in our synthesis of **IBR120**, we have employed catalytic stereoselective arylation methods to

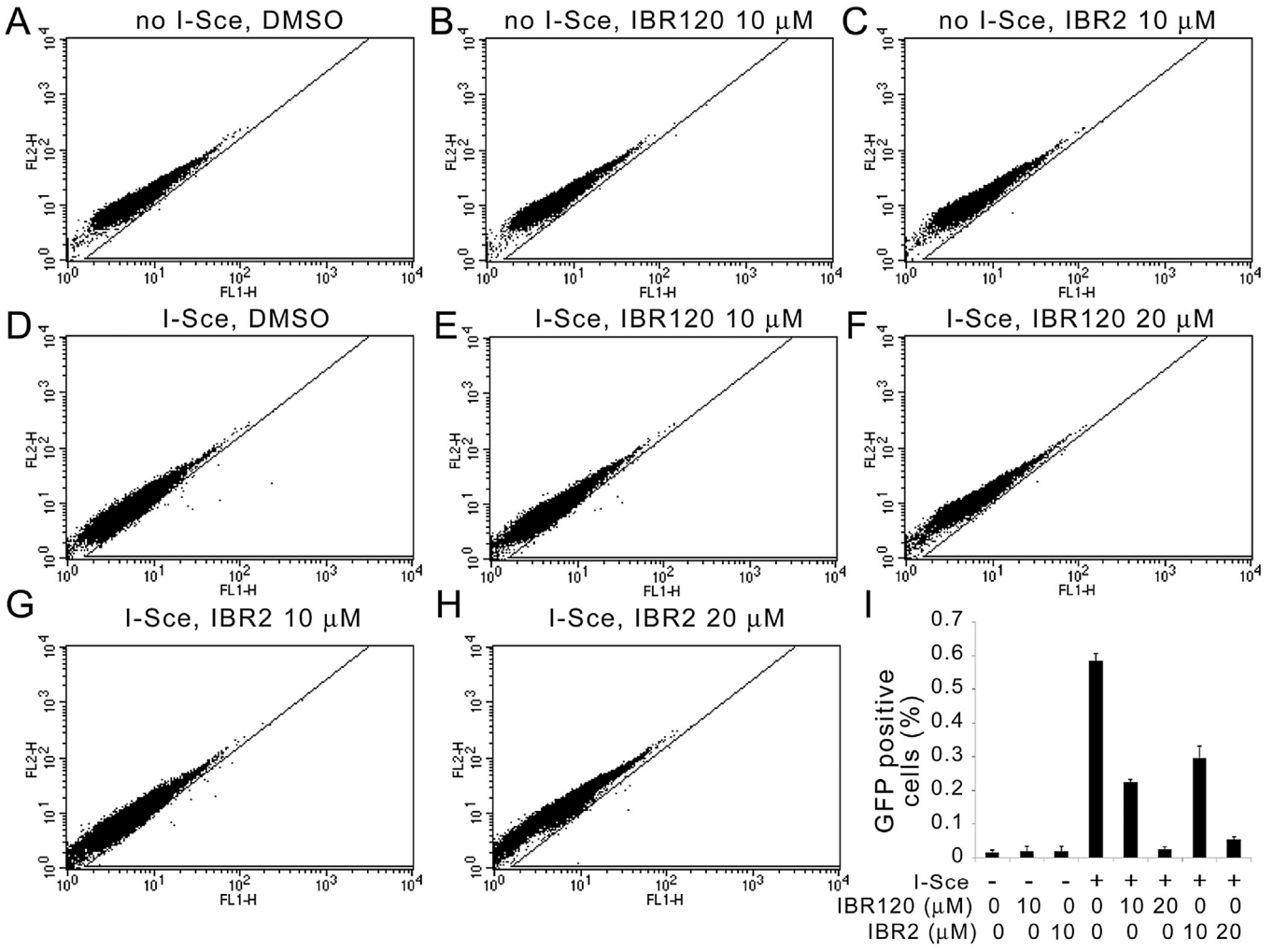


**Fig. 5. IBR120** dose dependently inhibits HR repair. HR frequency was measured by two-colour fluorescence flow cytometric analysis using HeLa-DR-GFP cells. Fifty thousand events were analyzed for each experiment. Cells were treated with DMSO (mock), 10 or 20 μM of IBR2 or IBR120 as indicated for 24 h after transient transfection with I-SceI expression vector pCABSce for 24 h. HR frequencies were indicated by GFP positive cell percentages. (A–H) Representative FACS analysis data for each treatment groups as indicated are shown in each panel. (I) Summary of HR frequency determined by FACS analysis. GFP positive cell percentages obtained by indicated treatments were from three independent experiments and summarized as means ± SD.

satisfactorily obtain the chiral starting material **24**, as previously described [17,18]. We have then improved the oxidation/reduction [20] and ring closure reactions to achieve moderate to high yields of the desired enantiomers. It is noteworthy that these steps were performed under very mild conditions, and could be telescoped with some adjustments, which is a very attractive feature of this synthetic route. With further optimization, next generation of **IBR120** analogues can be synthesized and screened for improved activity.

We have previously shown that **IBR2** directly target RAD51 both *in vitro* and in cells [15]. In this work, we demonstrate that **IBR120** can disrupt RAD51 multimer formation *in vitro*, and inhibit HR repair in cells, leading to growth inhibition and cell death. Our results indicate that **IBR120** has similar biochemical and cellular consequences as **IBR2**, and suggest they may share an identical molecular target. Notably, the central ring structure in **IBR120** is only one carbon smaller than that in **IBR2**, and this structural similarity suggests they might share similar pharmacokinetic and pharmacodynamic properties as well, which awaits further in-depth studies *in vivo*. With the quantitative structure-activity analysis in this work, further modifications are possible and necessary for this type of molecules to become clinically useful in the future.

**IBR120** showed consistent potency in various cancer cell lines with different cancer origins and genotypes, suggesting **IBR120** is an effective anti-cancer agent that might be used for various types of tumors. Taken together, we expect further improvement can be achieved based on these findings and may lead to the discovery and development of novel pharmaceutical strategies against difficult-to-treat cancers.

## 4. Experimental protocols

### 4.1. Cell lines and antibodies

Human leukemia cell line K562 and human breast cancer cell line T47D were maintained in RPMI 1640 (Invitrogen) supplemented with 10% fetal bovine serum (FBS) and 1% penicillin-streptomycin. Human breast cancer cell lines MCF7, MDA-MB-231, MDA-MB-361, MDA-MB-435, MDA-MB468, Hs578-T, human osteosarcoma cell line U2OS, human glioblastoma cell line T98G and human cervical adenocarcinoma cell line HeLa were maintained in low glucose Dulbecco Modified Eagle Medium (DMEM, Invitrogen) supplemented with 10% FBS and 1% penicillin-streptomycin. Human normal mammary epithelial cell line MCF10A was maintained in DMEM/F12 (50:50) medium (Invitrogen) supplemented with 5% horse serum, 20 ng/mL of epidermal growth factor, 0.5 mg/mL of hydrocortisone, 100 ng/mL of Cholera Toxin, 10 μg/mL of insulin, and 1% penicillin-streptomycin. To establish HeLa cells that stably expressed DR-GFP construct, cells were transfected with DR-GFP plasmid and selected with 2 μg/mL puromycin. Antibody sources were: mouse anti-RAD51 clone 14B4 and mouse anti-p84 (GeneTex), and secondary antibodies conjugated with Horseradish Peroxidase (GeneTex).

### 4.2. Cell killing assay

Standard XTT assays with a four-day drug treatment procedure were performed to measure the dose dependent cytotoxicity of IBR analogs in cultured cells. In brief, cells were plated on 96-well dishes one day before the drug treatment, followed by drug treatment on day 2 and XTT assay on day 6 after drug addition by using a commercial cell proliferation kit (Roche Scientific) following the instructions. Triplicate sets were measured and compiled for final data presentation.

### 4.3. Homologous recombination assay

As previously described [15], HeLa cells stably expressing DR-GFP were transfected with the I-Sce expression vector pCBASce and treated with compounds or DMSO. Cells were then trypsinized and subjected to flow cytometry. GFP positive cell percentages from three independent experiments were summarized as means ± SD.

### 4.4. Molecular modeling

The molecular docking was carried out following a previously established protocol [15]. RAD51 coordinates were from PDB (Accession No: 1N0W). RAD51 residues containing atoms within 5 Å distance from the BRC4 peptide in 1N0W was designated as binding site for docking, including residues M158, Y159, I160, F167, P168, L171, S183, V185, L186, D187, N188, V189, A190, Y191, A192, R193, A194, F195, H199, Q202, L203, L204, Y205, Q206, A207, S208, A209, M210, V212, E213, Y216, L219, R247, R250, M251, L252, R254, L255, E258, F259. Structures of small molecules were generated and optimized and molecular docking was performed using ICM Pro (Molsoft), following standard procedures as described by the software manual, using default docking parameters at thoroughness = 5. Docked conformations with RMSD < 2 Å were considered acceptable and kept for future analysis. Dihedral angles in the lowest energy docked conformation were recorded. Statistic analysis, clustering analysis, and predictive multivariate linear model building was performed using R (Version 3.1.0).

### 4.5. Multimer formation assay

Multimer formation assay was performed following a previously established protocol [15]. A mixture of RAD51 (3.2 μg) and IBR120 (1:10 M ratio) was incubated for 15 min at 37 °C, supplemented with buffer (50 mM triethanolamine-HCl [pH7.5], 0.5 mM $Mg(OAc)_2$, 1 mM DTT, 2 mM ATP and 100 μg/ml BSA, total volume 20 μl) and incubated for 15 min. The mixture was loaded onto a 2.4 ml Superdex 200 PC 3.2/30 column (Pharmacia) equilibrated with the same buffer as previously described [15]. Fractions (50 μl) were collected and 0.5 μl of each fraction was blotted onto PVDF membrane. RAD51 was detected using anti-RAD51 antibody (mAb 14B4, GeneTex).

### 4.6. Synthesis of IBR derivatives

#### 4.6.1. Material and methods

All reagents were used as received from commercial sources, unless specified otherwise, or prepared as described in the literature. Reactions requiring anhydrous conditions were performed in vacuum heat-dried glassware under nitrogen atmosphere. Reaction mixtures were stirred magnetically. DMF, dichloromethane and pyridine were distilled from $CaH_2$. $^1H$ NMR spectra were recorded at either 400 MHz or 500 MHz. $^{13}C$ NMR spectra were recorded at either 125 MHz or 100 MHz. Chemical shifts ($\delta$) are reported in ppm, and coupling constants ($J$) are in Hz. The following abbreviations were used to explain the multiplicities: s = singlet, d = doublet, t = triplet, q = quartet, m = multiplet.

#### 4.6.2. (R)-2-Methylpropane-2-sulfinic acid [[2-(2-benzyloxy-ethyl) phenyl]-(1H-indazol-3-yl)-methyl]amide (**6**)

The solution of compound **5** (1.34 g, 6.85 mmol) in THF (40 mL) was cooled to −78 °C and *n*-BuLi (1.6 M in hexane, 4.28 mL, 6.95 mmol) was added dropwise. The resultant solution was stirred at −78 °C for 5 min. After that, *t*-BuLi (1.7 M in pentane, 8.06 mL, 13.70 mmol) was added dropwise and the resultant solution was stirred for 15 min at −78 °C. Then, a solution of compound 2 [17]

(2.35 g, 6.85 mmol) in THF (8 mL) was added dropwise. The mixture was stirred for 1 h at −78 °C before saturated aqueous $NH_4Cl$ (3 mL) was added to quench the reaction. After the mixture was warmed up to room temperature, the mixture was poured to $H_2O$ (200 mL) and extracted with $CH_2Cl_2$ (3 × 60 mL). The combined organic phases were dried over anhydrous $Na_2SO_4$. The solvent was removed in vacuo and the resultant residue was purified by silica gel chromatography (hexane/EtOAc/$NH_3$ = 100: 50: 1) to give compound **6** (1.36 g, 43%) as a yellow foam. $^1$H NMR (500 MHz, $CDCl_3$) δ 7.43 (d, *J* = 8.0 Hz, 0.17H), 7.37–7.33 (m, 1.83H), 7.31–7.23 (m, 8H), 7.17–7.06 (m, 2H), 6.91 (t, *J* = 8.8 Hz, 0.83H), 6.83 (d, J = 9.0 Hz, 0.17H), 6.78 (t, *J* = 7.5 Hz, 0.17H), 6.73 (t, *J* = 8.0 Hz, 0.83H), 6.36 (d, *J* = 6.5 Hz, 0.83H), 6.24 (d, *J* = 2.5 Hz, 0.17H), 6.00 (d, *J* = 6.5 Hz, 1H), 4.48 (s, 1.66H), 4.28–4.22 (m, 0.34H), 3.78–3.69 (m, 1.66H), 3.46–3.41 (m, 0.34H), 3.33–3.23 (m, 1.66H), 3.20–3.07 (m, 0.34H), 1.29 (s, 1.5H), 1.27 (s, 7.5H); $^{13}$C NMR (125 MHz, $CDCl_3$) δ 144.9, 144.9, 141.5, 141.5, 139.5, 138.5, 138.4, 138.1, 136.5, 130.9, 130.3, 128.8, 128.5, 128.5, 128.4, 128.0, 127.8, 127.7, 127.7, 127.5, 126.9, 126.8, 126.5, 126.4, 120.9, 120.9, 120.5, 120.5, 120.4, 120.3, 110.7, 110.7, 73.2, 72.9, 71.1, 70.7, 56.9, 56.6, 54.5, 54.4, 33.0, 32.8, 23.4, 23.0; MS (ESI) *m/z* 484 (M + $Na^+$); HRMS Calcd for $C_{27}H_{31}N_3O_2SNa$ (M + $Na^+$), 484.2035 Found: 484.2021.

#### 4.6.3. 3-[(S)-[2-(2-Benzyloxyethyl)phenyl]-((R)-2-methylpropane-2-sulfinylamino)methyl]indazole-1-carboxylic acid tert-butyl ester (**7**) and 3-[(R)-[2-(2-Benzyloxyethyl)phenyl]-((R)-2-methylpropane-2-sulfinylamino)methyl]indazole-1-carboxylic acid tert-butyl ester (**8**)

To a 0 °C solution of compound **6** (706 mg, 1.53 mmol) in $CH_2Cl_2$ (20 mL) was added DMAP (5.0 mg, 0.04 mmol) followed by a solution of $Boc_2O$ (350 mg, 1.60 mmol) in $CH_2Cl_2$ (2.0 mL). The mixture was warmed up to room temperature and stirred for 1 h. Removal of all the solvent in vacuo resulted in a residue, which was purified by silica gel chromatography (hexane/EtOAc = 3: 1 to 2: 1) to give compound **8** (less polar, 117 mg, 14%) as an oil and compound **7** (more polar, 565 mg, 66%) as an oil.

Compound **7**: $[\alpha]_D^{20}$ = +7.3 (*c* 0.9 $CH_2Cl_2$); $^1$H NMR (500 MHz, $CDCl_3$) δ 8.13 (d, *J* = 9.0 Hz, 1H), 7.50 (d, *J* = 8.0 Hz, 1H), 7.44 (t, *J* = 8.0 Hz, 1H), 7.33–7.19 (m, 8H), 7.15–7.10 (m, 2H), 6.42 (d, *J* = 3.0 Hz, 1H), 4.54–4.48 (m, 2H), 4.28 (d, *J* = 3.0 Hz, 1H), 3.86–3.76 (m, 2H), 3.27 (t, *J* = 6.5 Hz, 2H), 1.70 (s, 9H), 1.25 (s, 9H); $^{13}$C NMR (125 MHz, $CDCl_3$) δ 150.9, 149.4, 141.2, 138.4, 138.2, 138.0, 130.8, 128.9, 128.7, 128.7, 128.5, 127.7, 127.6, 127.0, 124.3, 123.4, 121.7, 114.9, 84.7, 73.1, 70.9, 56.5, 54.1, 32.5, 28.4, 23.0; MS (ESI) *m/z* 584 (M + $Na^+$); HRMS Calcd for $C_{32}H_{39}N_3O_4SNa$ (M + $Na^+$), 584.2559 Found: 584.2560.

Compound **8**: $[\alpha]_D^{20}$ = −112 (*c* 1.1 $CH_2Cl_2$); $^1$H NMR (500 MHz, $CDCl_3$) δ 8.07 (d, *J* = 8.0 Hz, 1H), 7.39 (dd, *J* = 18.5, 7.5 Hz, 2H), 7.32–7.17 (m, 9H), 7.02–6.96 (m, 2H), 6.26 (d, *J* = 2.5 Hz, 1H), 4.44–4.36 (m, 2H), 3.69–3.61 (m, 2H), 3.29–3.23 (m, 1H), 3.16–3.10 (m, 1H), 1.71 (s, 9H), 1.25 (s, 9H); $^{13}$C NMR (125 MHz, $CDCl_3$) δ 150.8, 149.2, 141.2, 138.5, 138.4, 137.4, 130.8, 130.3, 129.0, 128.7, 128.5, 127.7, 127.6, 127.1, 123.8, 123.6, 121.2, 114.8, 84.8, 73.1, 70.9, 56.1, 53.4, 33.0, 28.4, 22.9; MS (ESI) *m/z* 584 (M + $Na^+$); HRMS Calcd for $C_{32}H_{39}N_3O_4SNa$ (M + $Na^+$), 584.2559 Found: 584.2559.

#### 4.6.4. 3-[(R)-Amino-[2-(2-benzyloxyethyl)phenyl]methyl]indazole-1-carboxylic acid tert-butyl ester (**9**)

To a solution of compound **8** (118 mg, 0.21 mmol) in MeOH (2.5 mL) was added 4 M HCl solution (in dioxane, 2.5 mL). After the mixture was stirred at room temperature for 30 min, the mixture was diluted with $H_2O$ (100 mL) and saturated aqueous $NaHCO_3$ (20 mL) was added. Then, the resultant aqueous solution was extracted with $CH_2Cl_2$ (3 × 30 mL). The combined organic layers were washed with brine, and then dried over anhydrous $Na_2SO_4$. After filtration and removal of the solvent in vacuo, the residue was purified by silica gel column chromatography ($CH_2Cl_2$/MeOH/$NH_3$ = 200: 10: 1) to afford compound **9** (87 mg, 90%) as a clear oil. $[\alpha]_D^{20}$ = −85 (*c* 1.0 $CH_2Cl_2$); $^1$H NMR (500 MHz, $CDCl_3$) δ 8.03 (d, *J* = 9.5 Hz, 1H), 7.41 (t, *J* = 7.3 Hz, 1H), 7.28–7.21 (m, 8H), 7.15–7.10 (m, 2H), 7.03 (t, *J* = 7.5 Hz, 1H), 5.89 (s, 1H), 4.51 (s, 2H), 3.78 (t, *J* = 8.0 Hz, 2H), 3.22 (t, *J* = 6.5 Hz, 2H), 2.98 (br, 2H), 1.73 (s, 9H); $^{13}$C NMR (125 MHz, $CDCl_3$) δ 154.0, 149.5, 140.9, 140.4, 138.3, 137.6, 130.6, 128.9, 128.6, 128.2, 128.0, 127.9, 127.8, 127.1, 124.1, 123.4, 121.5, 114.7, 85.0, 73.2, 71.3, 51.1, 33.1, 28.4; MS (ESI) *m/z* 480 (M + $Na^+$); HRMS Calcd for $C_{28}H_{32}N_3O_3$ (M + $H^+$), 458.2444 Found: 458.2424.

#### 4.6.5. 3-[(R)-Benzyloxycarbonylamino-[2-(2-hydroxyethyl)phenyl]methyl]indazole-1-carboxylic acid tert-butyl ester (**10**)

To a stirred solution of **9** (86 mg, 0.19 mmol) in MeOH (8 mL) was added 4 M HCl in dioxane (0.4 mL), followed by Pd/C (50 mg, 10% Pd). The mixture was hydrogenated at room temperature under 1 atm for 1 h. Then, the mixture was filtrated and the filtrate was neutralized with a $NaHCO_3$ aqueous solution. The resulted mixture was extracted with $CH_2Cl_2$ (3 × 30 mL). The combined organic layers were washed with brine, and then dried over anhydrous $Na_2SO_4$. After filtration and removal of the solvent in vacuo, the residue was solved in $CH_2Cl_2$ (3 mL) and the solvent was cooled to 0 °C. To this solvent was added DIPEA (40 μL, 0.23 mmol) followed by CbzCl (40 mg, 0.23 mmol) dropwise. The mixture was stirred at 0 °C for 20 min. Then, all the solvent was removed in vacuo and the residue was purified by silica gel chromatography (hexane/EtOAc = 2: 1) to give the compound **10** (57 mg, 61%) as a oil. $[\alpha]_D^{20}$ = −95 (*c* 0.9 $CH_2Cl_2$); $^1$H NMR (400 MHz, $CDCl_3$) δ 8.04 (d, *J* = 8.4 Hz, 1H), 7.44 (ddd, *J* = 8.4, 7.2, 4.2 Hz, 1H), 7.33–7.22 (m, 9H), 7.16–7.11 (m, 2H), 6.66 (d, *J* = 7.6 Hz, 1H), 6.55 (d, *J* = 6.4 Hz, 1H), 5.14–5.05 (m, 2H), 3.97 (br, 2H), 3.31–3.25 (m, 1H), 3.22–3.16 (m, 1H), 2.77 (br, 1H), 1.72 (s, 9H); $^{13}$C NMR (125 MHz, $CDCl_3$) δ 156.1, 150.6, 149.2, 140.9, 138.2, 137.6, 136.4, 130.7, 129.2, 128.7, 128.7, 128.6, 128.3, 128.2, 127.3, 123.8, 123.8, 120.8, 114.9, 85.3, 67.3, 63.8, 50.6, 35.9, 28.4; MS (ESI) *m/z* 524 (M + $Na^+$); HRMS Calcd for $C_{29}H_{31}N_3O_5Na$ (M + $H^+$), 524.2161 Found: 524.2156.

#### 4.6.6. 3-[(R)-Benzyloxycarbonylamino-[2-(2-methanesulfonyloxyethyl)phenyl]methyl]indazole-1-carboxylic acid tert-butyl ester (**11**)

The compound **10** (57 mg, 0.11 mmol) was dissolved in $CH_2Cl_2$ (3 mL) and DIPEA (40 μL, 0.23 mmol) were added. Then, MsCl (13 μL, 0.17 mmol) was added dropwise. The mixture was stirred at room temperature for 20 min. After that, the solvent was removed in vacuo and the residue was purified by silica gel column chromatography (hexane/EtOAc = 2: 1) to afford **11** (60 mg, 91%) as a white foam. $[\alpha]_D^{20}$ = −88 (*c* 0.8 $CH_2Cl_2$); $^1$H NMR (400 MHz, $CDCl_3$) δ 8.06 (d, *J* = 8.4 Hz, 1H), 7.47 (ddd, *J* = 8.4, 7.2, 1.2 Hz, 1H), 7.34–7.26 (m, 9H), 7.22–7.15 (m, 2H), 6.54 (d, *J* = 7.2 Hz, 1H), 6.41 (d, *J* = 6.8 Hz, 1H), 5.15–5.07 (m, 2H), 5.48–4.43 (m, 2H), 3.39 (s, 2H), 2.84 (s, 3H), 1.73 (s, 9H); $^{13}$C NMR (125 MHz, $CDCl_3$) δ 155.9, 150.1, 149.1, 140.9, 138.2, 136.4, 134.6, 131.0, 129.4, 129.2, 128.7, 128.7, 128.3, 128.2, 128.0, 124.0, 123.6, 120.7, 115.0, 85.5, 70.2, 67.3, 50.8, 37.3, 32.2, 28.4; MS (ESI) *m/z* 602 (M + $Na^+$); HRMS Calcd for $C_{30}H_{33}N_3O_7SNa$ (M + $Na^+$), 602.1937 Found: 602.1948.

#### 4.6.7. (R)-3-(1,2,3,4-Tetrahydro-isoquinolin-1-yl)indazole-1-carboxylic acid tert-butyl ester (**12**)

To a solution of compound **11** (60 mg, 0.10 mmol) in MeOH (4 mL) was added Pd/C (55 mg, 10% Pd). The mixture was hydrogenated at room temperature under 1 atm for 1 h. Then, the solvent was removed in vacuo and the residue was purified by silica gel column chromatography ($CH_2Cl_2$/MeOH/$NH_3$ = 150: 10: 1) to afford **12** (34 mg, 94%) as a foam. $[\alpha]_D^{20}$ = +106 (*c* 1.0 $CH_2Cl_2$); $^1$H NMR

(500 MHz, $CDCl_3$) $\delta$ 8.06 (d, $J$ = 9.0 Hz, 1H), 7.41 (ddd, $J$ = 7.5, 7.5, 0.8 Hz, 1H), 7.22–7.15 (m, 3H), 7.08 (dd, $J$ = 7.8, 7.5 Hz, 1H), 6.99 (t, $J$ = 7.5 Hz, 1H), 6.86 (d, $J$ = 8.0 Hz, 1H), 5.68 (s, 1H), 3.41–3.36 (m, 1H), 3.24–3.16 (m, 2H), 2.91–2.86 (m, 1H), 2.21 (br, 1H), 1.75 (s, 9H); $^{13}$C NMR (125 MHz, $CDCl_3$) $\delta$ 153.9, 149.6, 141.1, 135.4, 135.3, 129.4, 128.8, 127.8, 127.0, 126.2, 124.2, 123.5, 122.5, 114.8, 85.2, 56.4, 43.3, 30.0, 28.5; MS (ESI) *m/z* 372 (M + $Na^+$); HRMS Calcd for $C_{21}H_{23}N_3O_2Na$ (M + $Na^+$), 372.1688 Found: 372.1687.

#### 4.6.8. (R)-1-(1H-Indazol-3-yl)-2-phenylmethanesulfonyl-1,2,3,4-tetrahydro-isoquinoline (**IBR117**)

To a solution of compound **12** (34 mg, 0.097 mmol) in MeOH (1 mL) was added a solution of NaOMe (2.7 mg, 0.05 mmol) in MeOH (0.1 mL). The resultant mixture was stirred at room temperature for 3 h. $CH_2Cl_2$ (20 mL) and $H_2O$ (50 mL) were added to dilute the mixture and the aqueous phase was extracted with $CH_2Cl_2$ (3 × 25 mL). The combined organic layers were dried over anhydrous $Na_2SO_4$. Removal of all the solvent in vacuo gave a residue, which was dissolved in $CH_2Cl_2$ (1 mL). The resultant solution was cooled to 0 °C and DIPEA (22 μL, 0.13 mmol) was added. Then, a solution of $BnSO_2Cl$ (20 mg, 0.10 mmol) in $CH_2Cl_2$ (0.25 mL) was added dropwise. The mixture was stirred at 0 °C for 20 min. Removal of all the solvent gave a residue, which was purified by silica gel chromatography (hexane/EtOAc = 2: 1) to afford compound **IBR117** (24 mg, 61%) as a white foam. $[\alpha]_D^{20}$ = +93 (*c* 0.6 $CH_2Cl_2$); $^1$H NMR (500 MHz, $CDCl_3$) $\delta$ 10.43 (br, 1H), 7.56 (dd, $J$ = 8.3, 3.5 Hz, 1H), 7.50 (d, $J$ = 8.5 Hz, 1H), 7.40 (t, $J$ = 7.5 Hz, 1H), 7.26–7.10 (m, 5H), 7.07 (t, $J$ = 7.5 Hz, 2H), 6.97 (d, $J$ = 8.0 Hz, 1H), 6.79 (d, $J$ = 7.5 Hz, 2H), 6.63 (s, 1H), 4.07–3.97 (m, 2H), 3.52 (dd, $J$ = 14.0, 6.5 Hz, 1H), 3.28 (ddd, $J$ = 12.5, 12.0, 3.5 Hz, 1H), 3.02 (ddd, $J$ = 17.0, 11.5, 6.0 Hz, 1H), 2.77 (dd, $J$ = 17.0, 2.5 Hz, 1H); $^{13}$C NMR (125 MHz, $CDCl_3$) $\delta$ 146.7, 141.3, 134.1, 133.9, 130.7, 129.5, 128.8, 128.5, 128.5, 128.2, 127.6, 127.4, 126.6, 122.1, 121.8, 121.0, 110.2, 59.4, 53.2, 40.8, 29.1; MS (ESI) *m/z* 426 (M + $Na^+$); HRMS Calcd for $C_{23}H_{22}N_3O_2S$ (M + $H^+$), 404.1433 Found: 404.1430.

#### 4.6.9. 3-[(S)-Amino-[2-(2-benzyloxyethyl)phenyl]methyl]indazole-1-carboxylic acid tert-butyl ester (**13**)

Compound **13** (203 mg, 91%) was prepared as a clear oil using the same conditions as described for the compound **9**. $[\alpha]_D^{20}$ = +85 (*c* 1.0 $CH_2Cl_2$); $^1$H NMR (500 MHz, $CDCl_3$) $\delta$ 8.03 (d, $J$ = 8.5 Hz, 1H), 7.41 (t, $J$ = 9.5 Hz, 1H), 7.30–7.20 (m, 8H), 7.16–7.10 (m, 2H), 7.03 (t, $J$ = 7.5 Hz, 1H), 5.89 (s, 1H), 4.51 (s, 2H), 3.78 (t, $J$ = 7.3 Hz, 2H), 3.22 (t, $J$ = 7.0 Hz, 2H), 2.99 (br, 2H), 1.73 (s, 9H); $^{13}$C NMR (125 MHz, $CDCl_3$) $\delta$ 154.0, 149.5, 140.9, 140.4, 138.3, 137.6, 130.6, 128.9, 128.5, 128.2, 128.0, 127.9, 127.8, 127.1, 124.1, 123.4, 121.5, 114.7, 85.0, 73.2, 71.3, 51.1, 33.1, 28.4; MS (ESI) *m/z* 458 (M + $H^+$); HRMS Calcd for $C_{28}H_{32}N_3O_3$ (M + $H^+$), 458.2444 Found: 458.2435.

#### 4.6.10. 3-[(S)-Benzyloxycarbonylamino-[2-(2-hydroxyethyl)phenyl]methyl]indazole-1-carboxylic acid tert-butyl ester (**14**)

Compound **14** (159 mg, 71%) was prepared as a white foam using the same conditions as described for the compound **10**. $[\alpha]_D^{20}$ = +99 (*c* 0.9 $CH_2Cl_2$); $^1$H NMR (400 MHz, $CDCl_3$) $\delta$ 8.04 (d, $J$ = 8.4 Hz, 1H), 7.44 (ddd, $J$ = 8.4, 7.2, 1.2 Hz, 1H), 7.33–7.22 (m, 9H), 7.16–7.11 (m, 2H), 6.65 (d, $J$ = 7.2 Hz, 1H), 6.55 (d, $J$ = 6.4 Hz, 1H), 5.14–5.05 (m, 2H), 3.96 (br, 2H), 3.31–3.25 (m, 1H), 3.22–3.15 (m, 1H), 2.77 (br, 1H), 1.72 (s, 9H); $^{13}$C NMR (125 MHz, $CDCl_3$) $\delta$ 156.1, 150.6, 149.2, 140.9, 138.2, 137.6, 136.4, 130.7, 129.2, 128.7, 128.7, 128.6, 128.3, 128.2, 127.3, 123.8, 123.8, 120.8, 114.9, 85.3, 67.3, 63.8, 50.7, 35.9, 28.4; MS (ESI) *m/z* 524 (M + $Na^+$); HRMS Calcd for $C_{29}H_{31}N_3O_5Na$ (M + $Na^+$), 524.2161 Found: 524.2169.

#### 4.6.11. 3-[(S)-Benzyloxycarbonylamino-[2-(2-methanesulfonyloxyethyl)phenyl]methyl]indazole-1-carboxylic acid tert-butyl ester (**15**)

Compound **15** (161 mg, 88%) was prepared as a white foam using the same conditions as described for the compound **11**. $[\alpha]_D^{20}$ = +86 (*c* 1.2 $CH_2Cl_2$); $^1$H NMR (400 MHz, $CDCl_3$) $\delta$ 8.06 (d, $J$ = 8.4 Hz, 1H), 7.47 (ddd, $J$ = 8.4, 7.2, 0.8 Hz, 1H), 7.34–7.26 (m, 9H), 7.22–7.15 (m, 2H), 6.54 (d, $J$ = 7.2 Hz, 1H), 6.41 (d, $J$ = 5.6 Hz, 1H), 5.15–5.07 (m, 2H), 5.57–4.43 (m, 2H), 3.39 (s, 2H), 2.84 (s, 3H), 1.73 (s, 9H); $^{13}$C NMR (125 MHz, $CDCl_3$) $\delta$ 155.9, 150.1, 149.2, 140.9, 138.2, 136.4, 134.6, 131.0, 129.4, 129.2, 128.7, 128.7, 128.3, 128.2, 128.0, 124.0, 123.6, 120.7, 115.0, 85.4, 70.1, 67.3, 50.8, 37.3, 32.2, 28.4; MS (ESI) *m/z* 602 (M + $Na^+$); HRMS Calcd for $C_{30}H_{33}N_3O_7SNa$ (M + $Na^+$), 602.1937 Found: 602.1941.

#### 4.6.12. (S)-3-(1,2,3,4-Tetrahydro-isoquinolin-1-yl)indazole-1-carboxylic acid tert-butyl ester (**16**)

Compound **16** (95 mg, 97%) was prepared as a white foam using the same conditions as described for the compound **12**. $[\alpha]_D^{20}$ = −108 (*c* 0.7 $CH_2Cl_2$); $^1$H NMR (500 MHz, $CDCl_3$) $\delta$ 8.06 (d, $J$ = 8.5 Hz, 1H), 7.41 (ddd, $J$ = 7.5, 7.3, 0.8 Hz, 1H), 7.22–7.15 (m, 3H), 7.07 (t, $J$ = 7.5 Hz, 1H), 6.99 (t, $J$ = 4.0 Hz, 1H), 6.86 (d, $J$ = 8.0 Hz, 1H), 5.68 (s, 1H), 3.41–3.36 (m, 1H), 3.24–3.16 (m, 2H), 2.91–2.86 (m, 1H), 2.21 (br, 1H), 1.75 (s, 9H); $^{13}$C NMR (125 MHz, $CDCl_3$) $\delta$ 153.9, 149.5, 141.1, 135.4, 135.3, 129.4, 128.8, 127.7, 127.0, 126.1, 124.2, 123.5, 122.5, 114.8, 85.2, 56.4, 43.3, 29.9, 28.5; MS (ESI) *m/z* 350 (M + $H^+$); HRMS Calcd for $C_{21}H_{24}N_3O_2$ (M + $H^+$), 350.1869 Found: 350.1863.

#### 4.6.13. (S)-1-(1H-Indazol-3-yl)-2-phenylmethanesulfonyl-1,2,3,4-tetrahydro-isoquinoline (**IBR118**)

**IBR118** (73 mg, 67%) was prepared as white foam using the same conditions as described for the compound **IBR117**. $[\alpha]_D^{20}$ = −90 (*c* 0.8 $CH_2Cl_2$); $^1$H NMR (500 MHz, $CDCl_3$) $\delta$ 10.43 (br, 1H), 7.55 (dd, $J$ = 8.0, 3.0 Hz, 1H), 7.50 (d, $J$ = 8.5 Hz, 1H), 7.40 (t, $J$ = 7.0 Hz, 1H), 7.26–7.10 (m, 5H), 7.06 (t, $J$ = 7.0 Hz, 2H), 6.97 (d, $J$ = 8.0 Hz, 1H), 6.79 (d, $J$ = 7.5 Hz, 2H), 6.63 (s, 1H), 4.07–3.97 (m, 2H), 3.53 (dd, $J$ = 12.5, 6.5 Hz, 1H), 3.28 (ddd, $J$ = 12.5, 12.0, 3.5 Hz, 1H), 3.02 (ddd, $J$ = 18.0, 11.5, 6.0 Hz, 1H), 2.77 (dd, $J$ = 17.0, 3.0 Hz, 1H); $^{13}$C NMR (125 MHz, $CDCl_3$) $\delta$ 146.7, 141.3, 134.1, 140.0, 130.7, 129.5, 128.8, 128.5, 128.5, 128.2, 127.6, 127.4, 126.6, 122.1, 121.8, 121.0, 110.2, 59.4, 53.2, 40.8, 29.1; MS (ESI) *m/z* 426 (M + $Na^+$); HRMS Calcd for $C_{23}H_{21}N_3O_2SNa$ (M + $Na^+$), 426.1252 Found: 426.1252.

#### 4.6.14. [5-[(R)-[2-(2-Benzyloxyethyl)phenyl]-((R)-2-methylpropane-2-sulfinylamino)methyl]thiazol-2-yl]carbamic acid tert-butyl ester (**18**) and [5-[(S)-[2-(2-Benzyloxyethyl)phenyl]-((R)-2-methylpropane-2-sulfinylamino)methyl]thiazol-2-yl]carbamic acid tert-butyl ester (**19**)

A solution of compound **17** (390 mg, 1.40 mmol) in THF (8 mL) was cooled to −78 °C and *n*-BuLi (2.86 M, 1.22 mL, 3.50 mmol) was added slowly. The resultant mixture was stirred at −78 °C for 20 min. After that, a solution of compound 2 (480 mg, 1.40 mmol) in THF (4 mL) was added slowly. The mixture was stirred at −78 °C for 20 min. Saturated aqueous $NH_4Cl$ (5 mL) was added to quench the reaction and the mixture was warmed up to room temperature. $H_2O$ (50 mL) was added and the mixture was extracted with $CH_2Cl_2$ (3 × 30 mL). The combined organic phases were dried over anhydrous $Na_2SO_4$. Removal of the solvent in vacuo resulted in a residue, which was purified by silica gel chromatography (hexane/EtOAc/$NH_3$ = 100/200/0.6 to 100/200/3) to give compound **19** (less polar, 235 mg, 31%) as a foam and compound **18** (more polar, 60 mg, 7.9%) as a foam.

Compound **18**: $[\alpha]_D^{20}$ = −55.8 (*c* 0.88 $CH_2Cl_2$); $^1$H NMR (500 MHz, $CDCl_3$) $\delta$ 11.73 (s, 1H), 7.60 (d, $J$ = 8.0 Hz, 1H), 7.30–7.18 (m, 8H), 7.15 (s, 1H), 6.12 (d, $J$ = 2.5 Hz, 1H), 4.53–4.46 (m, 2H), 3.81 (d, $J$ = 2.5 Hz,

1H), 3.73–3.68 (m, 1H), 3.66–3.61 (m, 1H), 3.08–2.95 (m, 2H), 1.49 (s, 9H), 1.22 (s, 9H); $^{13}$C NMR (125 MHz, $CDCl_3$) $\delta$ 162.3, 153.0, 138.5, 138.5, 137.0, 135.1, 133.3, 130.8, 128.5, 128.3, 127.8, 127.8, 127.6, 127.2, 82.4, 73.2, 70.7, 56.2, 51.9, 33.2, 28.4, 22.9; MS (ESI) *m/z* 566 ($M + Na^+$); HRMS Calcd for $C_{28}H_{37}N_3O_4S_2Na$ ($M + Na^+$), 566.2123 Found: 566.2122.

Compound **19**: $[\alpha]_D^{20} = +3.5$ (*c* 0.83 $CH_2Cl_2$); $^1$H NMR (500 MHz, $CDCl_3$) $\delta$ 7.52 (d, $J = 7.0$ Hz, 1H), 7.29–7.18 (m, 9H), 7.11 (s, 1H), 6.06 (s, 1H), 4.49 (s, 2H), 4.00 (br, 1H), 3.68–3.60 (m, 2H), 3.02 (t, $J = 6.5$ Hz, 2H), 1.47 (s, 9H), 1.24 (s, 9H); $^{13}$C NMR (125 MHz, $CDCl_3$) $\delta$ 162.6, 152.8, 139.6, 138.3, 136.7, 132.8, 130.7, 128.6, 128.5, 127.8, 127.7, 127.5, 127.1, 82.5, 73.2, 70.6, 56.3, 52.9, 32.9, 28.4, 23.0; MS (ESI) *m/z* 566 ($M + Na^+$); HRMS Calcd for $C_{28}H_{37}N_3O_4S_2Na$ ($M + Na^+$), 566.2123 Found: 566.2128.

#### 4.6.15. (5-[(S)-Amino-[2-(2-benzyloxyethyl)phenyl]methyl]thiazol-2-yl)carbamic acid tert-butyl ester (**20**)

A solution of compound **19** (219 mg, 0.40 mmol) in MeOH (5 mL) was added 4 M HCl in dioxane (5 mL). The mixture was stirred at room temperature for 30 min. After that, the mixture was poured to an aqueous $NaHCO_3$ (2.0 g in 50 mL $H_2O$). The mixture was extracted with $CH_2Cl_2$ (3 × 30 mL). The combined organic phases were dried over anhydrous $Na_2SO_4$. Removal of the solvent in vacuo resulted in a residue, which was purified by silica gel chromatography ($CH_2Cl_2$/MeOH/$NH_3$ = 200/20/1) to afford compound **20** (178 mg, quant.) as an oil. $[\alpha]_D^{20} = +49.3$ (*c* 0.94 $CH_2Cl_2$); $^1$H NMR (500 MHz, $CDCl_3$) $\delta$ 7.51 (d, $J = 7.5$ Hz, 1H), 7.31–7.17 (m, 8H), 6.90 (s, 1H), 5.59 (s, 1H), 4.47 (s, 2H), 3.67–3.59 (m, 3H), 3.07–3.01 (m, 1H), 2.94–2.88 (m, 1H), 2.26 (br, 2H), 1.43 (s, 9H); $^{13}$C NMR (125 MHz, $CDCl_3$) $\delta$ 161.6, 153.0, 142.4, 138.3, 136.6, 136.2, 133.7, 130.3, 128.6, 127.8, 127.8, 127.8, 127.3, 126.6, 81.9, 73.3, 71.2, 49.7, 33.1, 28.4; MS (ESI) *m/z* 462 ($M + Na^+$); HRMS Calcd for $C_{24}H_{29}N_3O_3SNa$ ($M + Na^+$), 462.1827 Found: 462.1828.

#### 4.6.16. (5-[(S)-[2-(2-Benzyloxyethyl)phenyl] phenylmethanesulfonylamino-methyl]thiazol-2-yl)carbamic acid tert-butyl ester (**21**)

A solution of compound **20** (178 mg, 0.40 mmol) in $CH_2Cl_2$ (8 mL) was added DIPEA (116 μL, 0.65 mmol) and DMAP (8.0 mg, 0.066 mmol) at 0 °C. Then, a solution of $BnSO_2Cl$ (130 mg, 0.68 mmol) was added dropwise. The mixture was warmed up to room temperature and stirred for 20 min. Removal of the solvent in vacuo resulted in a residue, which was purified by silica gel chromatography (hexane/EtOAc = 2/1) to give compound **21** (232 mg, 97%) as a yellow oil. $[\alpha]_D^{20} = -33.6$ (*c* 1.26 $CH_2Cl_2$); $^1$H NMR (500 MHz, $CDCl_3$) $\delta$ 12.06 (s, 1H), 7.35 (td, $J = 7.5$, 1.5 Hz, 1H), 7.28–7.22 (m, 7H), 7.19–7.14 (m, 4H), 7.05 (s, 1H), 7.00 (d, $J = 7.0$ Hz, 2H), 6.77 (br, 1H), 5.84 (d, $J = 8.0$ Hz, 1H), 4.20–4.11 (m, 2H), 3.99 (s, 2H), 3.64 (dt, $J = 9.0$, 4.5 Hz, 1H), 3.48 (ddd, $J = 9.5$, 9.5, 4.5 Hz, 1H), 2.91 (ddd, $J = 14.5$, 9.3, 4.5 Hz, 1H), 2.67 (dt, $J = 14.5$, 5.0 Hz, 1H), 1.46 (s, 9H); $^{13}$C NMR (125 MHz, $CDCl_3$) $\delta$ 162.2, 153.0, 138.7, 138.3, 137.5, 135.1, 133.8, 132.8, 131.5, 131.1, 129.2, 129.1, 128.9, 128.7, 128.6, 128.2, 128.0, 127.3, 82.2, 73.1, 70.7, 59.9, 55.3, 33.1, 28.4; MS (ESI) *m/z* 616 ($M + Na^+$); HRMS Calcd for $C_{31}H_{35}N_3O_5S_2Na$ ($M + Na^+$), 616.1916 Found: 616.1909.

#### 4.6.17. (5-[(S)-[2-(2-Hydroxyethyl)phenyl] phenylmethanesulfonylamino-methyl]thiazol-2-yl)-carbamic acid tert-butyl ester (**22**)

To a solution of compound **21** (225 mg, 0.38 mmol) in MeOH (10 mL) was added Pd/C (10% Pd, 198 mg) and 4 M HCl in dioxane (0.5 mL). The, the mixture was hydrogenated (1atm) for 5 h. The mixture was subjected to filtration and the filtrate was poured to $H_2O$ (50 ml). Saturated aqueous $NaHCO_3$ (10 mL) was added and the mixture was extracted with $CH_2Cl_2$ (3 × 25 mL). The combined organic phases were dried over anhydrous $Na_2SO_4$. Removal of the solvent in vacuo resulted in a residue, which was purified by silica gel chromatography ($CH_2Cl_2$/MeOH = 15/1) to afford compound **22** (152 mg, 80%) as a foam. $[\alpha]_D^{20} = -41$ (*c* 0.58 $CH_2Cl_2$); $^1$H NMR (500 MHz, $CDCl_3$) $\delta$ 7.37 (t, $J = 7.0$ Hz, 2H), 7.32–7.24 (m, 4H), 7.20 (t, $J = 7.5$ Hz, 2H), 7.03 (d, $J = 7.5$ Hz, 2H), 6.97 (s, 1H), 6.50 (br, 1H), 5.96 (d, $J = 8.5$ Hz, 1H), 4.21 (d, $J = 14.0$ Hz, 1H), 4.07 (d, $J = 13.5$ Hz, 1H), 3.80 (dt, $J = 9.5$, 5.0 Hz, 1H), 3.71–3.65 (m, 1H), 2.81 (ddd, $J = 14.0$, 9.3, 5.5 Hz, 1H), 2.68 (dt, $J = 14.5$, 5.0 Hz, 1H), 1.46 (s, 9H); $^{13}$C NMR (125 MHz, $CDCl_3$) $\delta$ 162.0, 152.8, 139.1, 137.9, 135.3, 133.3, 131.6, 131.1, 129.3, 129.1, 128.7, 128.6, 127.5; 82.5, 64.1, 60.0, 54.7, 35.4, 28.4; MS (ESI) *m/z* 526 ($M + Na^+$); HRMS Calcd for $C_{24}H_{29}N_3O_5S_2Na$ ($M + Na^+$), 526.1447 Found: 526.1442.

#### 4.6.18. [5-((S)-2-Phenylmethanesulfonyl-1,2,3,4-tetrahydroisoquinolin-1-yl)thiazol-2-yl]carbamic acid tert-butyl ester (**23**)

To a solution of compound **22** (152 mg, 0.30 mmol) in $CH_2Cl_2$ (5 mL) was added DMAP (3.0 mg, 0.025 mmol) and DIPEA (63 μL, 0.36 mmol) at 0 °C. Then, MsCl (80 μL, 1.03 mmol) was added dropwise. The mixture was stirred at room temperature for 20 min. After that, the solvent was removed in vacuo to afford a residue, which was purified by gel chromatography ($CH_2Cl_2$/MeOH = 30/1) to give a foam (168 mg). The yielded foam (168 mg) was dissolved in THF (10 mL) and the solution was cooled to 0 °C. To this solution was added KHMDS (0.5 M in toluene, 1.15 mL, 0.58 mmol) and the mixture was stirred at 0 °C for 5 min. The reaction was quenched with aqueous saturated $NH_4Cl$ (5 mL) and $H_2O$ (30 mL) was added. The mixture was extracted with $CH_2Cl_2$ (3 × 25 mL) and the combined organic phases were dried over anhydrous $Na_2SO_4$. The solvent was removed in vacuo and the resultant residue was purified by silica gel chromatography (hexane/EtOAc = 2/1) to give compound **23** (118 mg, 81%) as a foam. $[\alpha]_D^{20} = -50.7$ (*c* 0.63 $CH_2Cl_2$); $^1$H NMR (500 MHz, $CDCl_3$) $\delta$ 11.92 (s, 1H), 7.27–7.24 (m, 1H), 7.21–7.17 (m, 3H), 7.14–7.09 (m, 5H), 6.97 (d, $J = 7.0$ Hz, 1H), 6.08 (s, 1H), 4.13–4.08 (m, 2H), 3.63 (dd, $J = 14.0$, 6.0 Hz, 1H), 3.29 (ddd, $J = 15.5$, 10.5, 3.0 Hz, 1H), 2.82 (ddd, $J = 16.5$, 12.0, 5.0 Hz, 1H), 2.67 (dt, $J = 15.0$, 3.0 Hz, 1H), 1.47 (s, 9H); $^{13}$C NMR (125 MHz, $CDCl_3$) $\delta$ 162.5, 152.9, 136.8, 134.0, 133.5, 132.4, 130.9, 129.5, 128.8, 128.7, 128.7, 128.2, 127.9, 126.6, 82.4, 59.6, 53.4, 39.9, 29.9, 28.5; MS (ESI) *m/z* 508 ($M + Na^+$); HRMS Calcd for $C_{24}H_{27}N_3O_4S_2Na$ ($M + Na^+$), 508.1341 Found: 508.1344.

#### 4.6.19. 5-((S)-2-Phenylmethanesulfonyl-1,2,3,4-tetrahydro-isoquinolin-1-yl)thiazol-2-ylamine (***IBR119***)

To a solution of compound **23** (106 mg, 0.22 mmol) in $CH_2Cl_2$ (10 mL) was added TFA (1 mL) at 0 °C. The mixture was warmed up to room temperature and stirred for 5 h. $CH_2Cl_2$ (20 mL) and $H_2O$ (30 mL) were added to the reaction mixture. The reaction was quenched with aqueous saturated $NH_4Cl$ (5 mL) and $H_2O$ (30 mL) was added. After saturated aqueous $NaHCO_3$ (10 ml) was added, the mixture was extracted with $CH_2Cl_2$ (3 × 20 mL) and the combined organic phases were dried over anhydrous $Na_2SO_4$. The solvent was removed in vacuo and the resultant residue was purified by silica gel chromatography (hexane/EtOAc/$NH_3$ = 1: 1: 0 to 1: 2: 0.005) to give compound **IBR119** (73 mg, 87%) as a foam. $[\alpha]_D^{20} = -62.9$ (*c* 0.43 $CH_2Cl_2$); $^1$H NMR (500 MHz, $CDCl_3$) $\delta$ 7.19–7.26 (m, 1H), 7.24–7.19 (m, 3H), 7.16–7.10 (m, 4H), 6.98 (d, $J = 8.0$ Hz, 1H), 6.61 (s, 1H), 5.93 (s, 1H), 5.07 (br, 2H), 4.19–4.10 (m, 2H), 3.62 (dd, $J = 14.3$, 6.0 Hz, 1H), 3.22 (ddd, $J = 15.5$, 10.5, 3.5 Hz, 1H), 2.78 (ddd, $J = 17.8$, 11.3, 5.0 Hz, 1H), 2.66 (dd, $J = 16.5$, 1.5 Hz, 1H); $^{13}$C NMR (125 MHz, $CDCl_3$) $\delta$ 169.1, 138.9, 133.8, 133.6, 130.9, 129.4, 129.3, 128.8, 128.7, 128.7, 128.3, 127.9, 126.5, 59.8, 53.7, 39.6, 29.9; MS (ESI) *m/z* 386 ($M + H^+$); HRMS Calcd for $C_{19}H_{20}N_3O_2S_2$ ($M + H^+$), 386.0997 Found: 386.0996.

*4.6.20. (R)-N-((2-(hydroxymethyl)phenyl) (1H-indol-3-yl)methyl)-1-phenylmethanesulfonamide (**25**)*

To a solution of compound **24** [17] (176 mg, 0.44 mmol) in dioxane-water (3:1, 8 mL) were added 2, 6-lutidine (0.101 mL, 0.88 mmol), $OsO_4$ (2.5% in tert-butanol, 89 μL, 8.8 μmol) and $NaIO_4$ (371.4 mg, 1.75 mmol). The reaction was stirred at r.t and monitored by TLC. After the reaction was complete, water (10 mL) and $CH_2Cl_2$ (20 mL) were added. The organic layer was separated, and the water layer was extracted by $CH_2Cl_2$ (10 mL x 3). The combined organic layers were washed with brine and dried over $Na_2SO_4$. The solvent was removed under reduced pressure. The residue was absorbed onto $SiO_2$, and eluted with EtOAc/hexane (1:3) to afford the aldehyde intermediate as white foam (158 mg). This foam was dissolved in THF-MeOH (1:1, 4 mL) at 0 °C and $NaBH_4$ (44 mg, 1.17 mmol) in THF (1 mL) was added. The reaction was stirred for 10 min at room temperature and saturated aqueous $NH_4Cl$ (3 mL) was added to quench the reaction. $H_2O$ (30 mL) was added and the mixture was extracted with $Et_2O$ (3 × 20 mL). The combined organic phases were dried with anhydrous $Na_2SO_4$. The solvent was removed under reduced pressure and the residue was absorbed onto silica gel and eluted with hexane/EtOAc (1: 2) to give compound **25** (146 mg, 82%) as a foam. $[\alpha]_D^{20} = +70.2$ (*c* 1.06 $CH_2Cl_2$); $^1$H NMR (400 MHz, $CD_2Cl_2$) $\delta$ 8.26 (s, 1H), 7.62 (d, $J$ = 7.5 Hz, 1H), 7.36–7.52 (m, 6H), 7.15–7.31 (m, 4H), 7.02–7.04 (d, $J$ = 7.5 Hz, 2H), 6.94 (s, 1H), 6.27 (d, $J$ = 7.5 Hz, 1H), 5.76 (d, $J$ = 7.8 Hz, 1H), 4.47–4.57 (m, 2H), 4.13 (d, $J$ = 13.8 Hz, 1H), 4.02 (d, $J$ = 13.8 Hz, 1H), 1.80 (t, $J$ = 6.0 Hz, 1H); $^{13}$C NMR (100 MHz, $CDCl_3$) $\delta$ 140.1, 138.2, 136.9, 130.9, 130.7, 129.1, 129.0, 128.9, 128.7, 128.6, 128.6, 128.6, 125.5, 123.8, 122.6, 120.1, 119.6, 116.0, 111.6, 63.3, 60.1, 53.8; MS (ESI) *m/z* 429 (M + $Na^+$); HRMS Calcd for $C_{23}H_{22}N_2O_3SNa$ (M + $Na^+$), 429.1249 Found:429.1230.

*4.6.21. (R)-3-(2-(benzylsulfonyl)isoindolin-1-yl)-1h-indole (**IBR120**)*

To a stirred solution of compound **25** (28 mg, 0.069 mmol) in $CH_2Cl_2$ (2.0 mL) was added $Et_3N$ (9.6 μL, 0.069 mmol) at 0 °C. Then, MsCl (7.1 μL, 0.092 mmol) was added dropwise. The mixture was warmed up to room temperature and stirred for 1 h. The reaction solution was diluted with $CH_2Cl_2$ (5 ml) and washed with ice water. Organic phases were dried with anhydrous $Na_2SO_4$ and removed under vacuum. The residue was then dissolved in dry MeCN (2 mL) and to this solution was added DIPEA dropwise at 0 °C. The reaction was allowed warm up to r.t and monitored by TLC. After the reaction was completed, saturated aqueous $NH_4Cl$ (1 mL) was added and the mixture was extracted with $CH_2Cl_2$ (3 × 5 mL). The combined organic phases were dried over anhydrous $Na_2SO_4$. Removal of the solvent in vacuo resulted in a residue, which was purified by silica gel chromatography (EtOAc/hexane = 1: 3) to give compound **IBR120** (14.2 mg, 53%) as a white solid. $[\alpha]_D^{20} = +89.5$ (*c* 0.44 $CH_2Cl_2$); $^1$H NMR (400 MHz, $CD_2Cl_2$) $\delta$ 8.40 (s, 1H), 7.37–7.42 (m, 2H), 7.31–7.37 (t, $J$ = 7.3 Hz, 1H), 7.21–7.30 (m, 3H), 7.13–7.19 (m, 3H), 7.03–7.07 (d, $J$ = 7.6 Hz, 1H), 6.85–6.97 (m, 4H), 6.41 (d, $J$ = 1.8 Hz, 1H), 4.86 (d, $J$ = 13.3 Hz, 1H), 4.38–4.42 (dd, $J$ = 2.8, 13.6 Hz, 1H), 3.75 (d, $J$ = 13.6 Hz, 1H), 3.64 (d, $J$ = 13.7 Hz, 1H); $^{13}$C NMR (125 MHz, $CD_2Cl_2$) $\delta$ 140.7, 137.4, 136.5, 131.2, 129.7, 128.8, 128.7, 128.5, 128.4, 125.9, 125.7, 124.0, 122.9, 122.8, 120.4, 120.1, 116.0, 112.1, 63.2, 59.5, 54.2; MS (ESI) *m/z* 411 (M + $Na^+$); HRMS Calcd for $C_{23}H_{20}N_2O_2SNa$ (M + $Na^+$), 411.1143 Found: 411.1134.

*4.6.22. (S)-3-(2-(benzylsulfonyl)isoindolin-1-yl)-1H-indole (**IBR121**)*

**IBR121** (13.6 mg, 51%) was prepared as white solid using the same conditions as described for the compound IBR120. $[\alpha]_D^{20} = -90.1$ (*c* 0.75 $CH_2Cl_2$); $^1$H NMR (400 MHz, $CD_2Cl_2$) $\delta$ 8.37 (s, 1H), 7.39–7.42 (m, 2H), 7.32–7.35 (m, 1H), 7.22–7.28 (m, 3H), 7.13–7.17 (m, 3H), 7.03–7.05 (d, $J$ = 7.7 Hz, 1H), 6.85–6.96 (m, 4H), 6.41 (s, 1H), 4.85 (d, $J$ = 13.3 Hz, 1H), 4.37 (d, $J$ = 13.8 Hz, 1H), 3.74 (d, $J$ = 13.5 Hz, 1H), 3.63 (d, $J$ = 13.6 Hz, 1H); $^{13}$C NMR (125 MHz, $CD_2Cl_2$) $\delta$ 140.7, 137.3, 136.4, 131.2, 129.7, 128.7, 128.7, 128.4, 128.4, 125.7, 124.0, 122.9, 122.8, 120.4, 120.1, 116.0, 112.1, 63.1, 59.5, 54.2; MS (ESI) *m/z* 411 (M + $Na^+$); HRMS Calcd for $C_{23}H_{20}N_2O_2SNa$ (M + $Na^+$), 411.1143 Found: 411.1150.

## Acknowledgment

This work is supported by NIH grant to W.-H. Lee (CA107568). We thank the UCI Molecular Modeling Facility for technical support.

## Appendix A. Supplementary data

Supplementary data related to this article can be found at http://dx.doi.org/10.1016/j.ejmech.2015.04.021.

## References

[1] J.F. Carvalho, R. Kanaar, Targeting homologous recombination-mediated DNA repair in cancer, Expert Opin. Ther. Targets 18 (2014) 427–458.
[2] X.E. Guo, B. Ngo, A.S. Modrek, W.-H. Lee, Targeting tumor suppressor networks for Cancer therapeutics, Curr. Drug Targets 15 (2014) 2–16.
[3] A. Ward, K.K. Khanna, A.P. Wiegmans, Targeting homologous recombination, new pre-clinical and clinical therapeutic combinations inhibiting RAD51, Cancer Treat. Rev. 41 (2014) 35–45.
[4] N.J. Curtin, DNA repair dysregulation from cancer driver to therapeutic target, Nat. Rev. Cancer. 12 (2012) 801–817.
[5] J. Flygare, S. Fält, J. Ottervald, J. Castro, Å.-L. Dackland, D. Hellgren, A. Wennborg, Effects of HsRad51 overexpression on cell proliferation, cell cycle progression, and apoptosis, Exp. Cell. Res. 268 (2001) 61–69.
[6] C.-F. Chen, P.-L. Chen, Q. Zhong, Z.D. Sharp, W.-H. Lee, Expression of BRC repeats in breast Cancer cells disrupts the BRCA2-Rad51 complex and leads to radiation hypersensitivity and loss of G2/M checkpoint control, J. Biol. Chem. 274 (1999) 32931–32935.
[7] P.-L. Chen, C.-F. Chen, Y. Chen, J. Xiao, Z.D. Sharp, W.-H. Lee, The BRC repeats in BRCA2 are critical for RAD51 binding and resistance to methyl methanesulfonate treatment, Proc. Natl. Acad. Sci. U. S. A. 95 (1998) 5287–5292.
[8] H.L. Klein, The consequences of Rad51 overexpression for normal and tumor cells, DNA Repair 7 (2008) 686–693.
[9] H. Maacke, K. Jost, S. Opitz, S. Miska, Y. Yuan, L. Hasselbach, J. Luttges, H. Kalthoff, H.-W. Sturtzbecher, DNA repair and recombination factor Rad51 is over-expressed in human pancreatic adenocarcinoma, Oncogene 19 (2000) 2791–2795.
[10] G.-B. Qiao, Y.-L. Wu, X.-N. Yang, W.-Z. Zhong, D. Xie, X.-Y. Guan, D. Fischer, H.-C. Kolberg, S. Kruger, H.-W. Stuerzbecher, High-level expression of Rad51 is an independent prognostic marker of survival in non-small-cell lung cancer patients, Br. J. Cancer 93 (2005) 137–143.
[11] E. Raderschall, K. Stout, S. Freier, V. Suckow, S. Schweiger, T. Haaf, Elevated levels of Rad51 recombination protein in tumor cells, Cancer Res. 62 (2002) 219–225.
[12] C. Richardson, J.M. Stark, M. Ommundsen, M. Jasin, Rad51 overexpression promotes alternative double-strand break repair pathways and genome instability, Oncogene 23 (2004) 546–553.
[13] M.E. Robu, R.B. Inman, M.M. Cox, RecA protein promotes the regression of stalled replication forks in vitro, Proc. Natl. Acad. Sci. U. S. A. 98 (2001) 8211–8218.
[14] A. Slupianek, C. Schmutte, G. Tombline, M. Nieborowska-Skorska, G. Hoser, M.O. Nowicki, A.J. Pierce, R. Fishel, T. Skorski, BCR/ABL regulates mammalian RecA homologs, resulting in drug resistance, Mol. Cell. 8 (2001) 795–806.
[15] J. Zhu, L. Zhou, G. Wu, H. Konig, X. Lin, G. Li, X.-L. Qiu, C.-F. Chen, C.-M. Hu, E. Goldblatt, R. Bhatia, A.R. Chamberlin, P.-L. Chen, W.-H. Lee, A novel small molecule RAD51 inactivator overcomes imatinib-resistance in chronic myeloid leukaemia, EMBO Mol. Med. 5 (2013) 1–13.
[16] I.K. Reddy, R. Mehvar, Chirality in Drug Design and Development, first ed., CRC Press, 2004.
[17] X.-L. Qiu, J. Zhu, G. Wu, W.-H. Lee, A.R. Chamberlin, Stereoselective synthesis of chiral IBR2 analogues, J. Org. Chem. 74 (2009) 2018–2027.
[18] Y.-Q. Wang, J. Song, R. Hong, H. Li, L. Deng, Asymmetric Friedel-crafts reaction of indoles with imines by an organic catalyst, J. Am. Chem. Soc. 128 (2006) 8156–8157.
[19] W.M. Welch, C.E. Hanau, W.M. Whalen, A novel synthesis of 3-substituted indazole derivatives, Synthesis (1992) 937–939.
[20] W. Yu, Y. Mei, Y. Kang, Z. Hua, Z. Jin, Improved procedure for the oxidative cleavage of Olefins by $OsO_4$/$NaIO_4$, Org. Lett. 6 (2004) 3217–3219.
[21] C.A. Hudis, L. Gianni, Triple-negative breast Cancer: an Unmet medical need,

Oncology 16 (2011) 1–11.
[22] P.F. Peddi, M.J. Ellis, C. Ma, Molecular basis of triple negative breast Cancer and implications for therapy, Int. J. Breast Cancer. 2012 (2012) 1–7.
[23] ATCC Cell Lines – ATCC: The Global Bioresource Center, http://www.atcc.org.
[24] L. Pellegrini, D.S. Yu, T. Lo, S. Anand, M. Lee, T.L. Blundell, A.R. Venkitaraman, Insights into DNA recombination from the structure of a RAD51-BRCA2 complex, Nature 420 (2002) 287–293.
[25] A.J. Pierce, R.D. Johnson, L.H. Thompson, M. Jasin, XRCC3 promotes homology-directed repair of DNA damage in mammalian cells, Genes. Dev. 13 (1999) 2633–2638.